Renewable and Sustainable Energy Reviews 16 (2012) 2696–2723

Contents lists available at SciVerse ScienceDirect

Renewable and Sustainable Energy Reviews

journal homepage: www.elsevier.com/locate/rser

Organic light emitting diodes: Energy saving lighting technology—A review

N. Thejo Kalyani[a], S.J. Dhoble[b,*]

[a] Department of Applied Physics, Priyadarshini College of Engineering, Nagpur 440019, India
[b] Department of Physics, Rashatrasant Tukadoji Maharaj Nagpur University, Nagpur 440033, India

ARTICLE INFO

Article history:
Received 19 June 2011
Received in revised form 6 February 2012
Accepted 10 February 2012
Available online 22 March 2012

Keywords:
Luminescence
OLEDs
Energy saving
Eco-friendly
Fabrication technologies
Rare earths β-diketonates
Organic complexes
Solid-state lighting

ABSTRACT

This paper reflects the achievements and the challenges ahead in the field of organic light emitting diodes (OLEDs). The primary intention of this paper is to study different organic materials synthesized so far and the OLEDs fabricated for solid-state lighting. After deep review of literature we have synthesized and characterized rare earth based europium organic complexes $Eu(TTA)_3Phen$, $Eu_{(x)}Y_{(1-x)}(TTA)_3Phen$, and $Eu_{(x)}Tb_{(1-x)}(TTA)_3Phen$, where $x = 0.4$ and 0.5 by solution technique maintaining stoichiometric ratio. Blended films of pure and doped Eu complexes that are molecularly doped into polymer resins namely polymethylmethacrylate (PMMA) and polystyrene (PS) are prepared according to weight percentage. Concentration effect on absorption and emission spectra of the blended films was studied for different weight percentages (10, 25, 50, 60%). All the complexes doped in PMMA showed an excellent transparency of 90–97% while the complexes doped in polystyrene showed a transparency of 85–90%, bit less than in PMMA. Energy gap of the synthesized complexes have been determined in PMMA and PS. Considering the facts that these complexes have good solubility in most of the organic solvents, the absorption spectra of $Eu(TTA)_3Phen$, $Eu_{0.5}Y_{0.5}(TTA)_3Phen$ and $Eu_{0.5}Tb_{0.5}(TTA)_3Phen$ complexes are studied, and OLED devices having the structure ITO/m-MTDATA/α-NPD/TPBi:$Eu_{(x)}Y_{(1-x)}(TTA)_3Phen$/$Alq_3$/LiF:Al (where $x = 0.4$, 0.5) were fabricated and characterized. Significant red emission was observed from fabricated OLED devices at 612 nm when operated in a range of 10–18 V. Thus the synthesized rare earth based organic complexes are the best suitable candidates for fabrication of red OLED devices. The extensive review on OLEDS concludes that our present lighting system can be replaced with white OLEDS, recently developed energy saving lighting technology.

Contents

* Corresponding author. Tel.: +91 0712 2250180/2251361/2500083; mobile +91 9822710204.
E-mail address: sjdhoble@rediffmail.com (S.J. Dhoble).

1364-0321/$ – see front matter
doi:10.1016/j.rser.2012.02.021

1. Introduction

Even in this digital era one of the world major problems is the shortage of electricity. This is because of the present lighting system, which includes tungsten filament bulbs which consume more power, fluorescent lamps, which are not eco-friendly as they are excited by mercury, which is harmful, non-disposable, life time is only of the order 1000 h. Around 33% of electricity is utilized due to the present lighting system. In contrast the use of OLEDs, the new star of small screen, which is self-illuminating, eco-friendly and power saving for even solid-state lighting instead of the present lighting system could solve this problem to certain extent. These are extremely thin, flexible, varying in shapes, colors and sizes, some are even transparent while providing a lovely ambient glow. For solid-state lighting, one of the most studied devices is the light emitting diode whose light emissions originate from small organic molecules (OLEDs) or from semiconducting polymers (PLEDs). However, interest in developing PLEDs is rapidly growing, since the manufacturing technologies are solution based ink-jet printing, spin coating, etc., and are therefore much cheaper than traditional evaporation techniques used for OLEDs. In order to build full-color displays, pure blue, green, and red emissions are required and hence this review.

A great challenge in the field of organic light emitting diodes (OLEDs) is the realization of an efficient pure light emission from the diode with narrow emission line. Such an emitter is essential to complete the color spectrum for a full color display based on the principle of additive color mixing. One way to solve the problem is to use an organic Eu^{3+} complex in which Eu^{3+} ions acts as the emission centre [1–6]. The spectral properties of Eu^{3+} are ideal for use in full color displays as known from inorganic luminescent materials in cathode ray and projection television tubes. To design a red emitting OLED based on Eu^{3+} complex two criteria have to be fulfilled:

(i) The Eu^{3+} complex has to exhibit a high fluorescence quantum efficiency and
(ii) The Eu^{3+} complex has to be integrated in the OLED structure such that high electro luminescence efficiency is achieved.

Now the only area remaining where large improvements to efficiency can be made that of extracting more of the light that is trapped within the device, a challenging problem from both the scientific and technological point of view, but if successful will lead to a major and commercially important advance in OLED displays.

1.1. *Basics of luminescence*

Light is a form of energy. To create light, another form of energy must be supplied. There are two common ways for this to occur, incandescence and luminescence. Incandescence is light from heat energy. If you heat something to a high enough temperature, it will begin to glow. For example, when an electric stove's heater or metal in a flame begin to glow "red hot" that is incandescence. When the tungsten filament of an ordinary incandescent light bulb is heated still hotter, it glows brightly "white hot" by the same means. The sun and stars glow by incandescence. Luminescence, general term applied to all forms of cool light, i.e., light emitted by sources other than a hot, incandescent body, such as a black body radiator. Luminescence is caused by the movement of electrons within a substance from more energetic states to less energetic states. There are many types of luminescence, including chemiluminescence, produced by certain chemical reactions, chiefly oxidations, at low temperatures; electroluminescence, produced by electric discharges, which may appear when silk or fur is stroked or when adhesive surfaces are separated; triboluminescence, produced by rubbing or crushing crystals. Bioluminescence is produced by living microscopic organisms, which collect at the surface of the sea. If the luminescence is caused by absorption of some form of radiant energy, such as ultraviolet radiation or X rays (or by some other form of energy, such as mechanical pressure), and ceases as soon as (or very shortly after) the radiation causing it ceases, then it is known as fluorescence. If the luminescence continues after the radiation causing it has stopped, then it is known as

phosphorescence. Luminescence of inorganic and organic substances results from an emission transition of anions, molecules or a crystal from an excited electronic state to a ground state with lesser energy. In fluorescence, the luminescence emission has a lifetime $<10^{-8}$ s, while in phosphorescence the luminescence emission has a lifetime $>10^{-8}$ s.

1.1.1. Fluorescence

The phenomenon known as fluorescence occurs at the subatomic level by a process called electron excitation. Electrons are subatomic particles that orbit the nucleus of an atom at specific distances known as electron shells. These shells are arranged in layers around the nucleus, the exact number of electrons and their shells depending on the type of atom (element). The electrons contained in the shells nearest the nucleus carry less energy than the electrons in the outer shells. When certain atoms are exposed to ultraviolet (UV) light, a photon (particle of light energy) of UV will cause an electron residing in a lower-energy inner electron shell to be temporarily boosted to a higher-energy outer shell. When this occurs the electron is said to be "excited." It will then drop back to its original inner electron shell, releasing its extra energy in the form of a photon of visible light. This visible light is the fluorescent color that our eyes perceive. The exact color depends on the wavelength of the visible light emitted, with the wavelength itself being dependent on the type of atom undergoing the electron excitation.

$$\text{Excitation} : S_0 = h\nu_{\text{ext}} + S_1$$

$$\text{Fluorescence (emission)} : S_1 \rightarrow S_0 + h\nu_{\text{em}} + \text{heat}$$

Here $h\nu$ is a generic term for photon energy with h = Planck's constant and ν = frequency of light (the specific frequencies of exciting and emitted light are dependent on the particular system). State S_0 is called the ground state of the fluorophore (fluorescent molecule) and S_1 is its first (electronically) excited state. A molecule in its excited state S_1, can relax by various competing pathways. It can undergo 'non-radiative relaxation' in which the excitation energy is dissipated as heat to the solvent. Excited organic molecules can also relax via conversion to a triplet state, which may subsequently relax via phosphorescence or by a secondary non-radiative relaxation step. Relaxation of an S_1 state can also occur through interaction with a second molecule through fluorescence quenching. Molecular oxygen (O_2) is an extremely efficient quencher of fluorescence just because of its unusual triplet ground state.

The fluorescence quantum yield gives the efficiency of the fluorescence process. It is defined as the ratio of the number of photons emitted to the number of photons absorbed. The maximum fluorescence quantum yield is 1.0 (100%); every photon absorbed results in a photon emitted. Compounds with quantum yields of 0.10 are still considered quite fluorescent.

The fluorescence lifetime refers to the average time the molecule stays in its excited state before emitting a photon. Fluorescence typically follows first-order kinetics: $[S_1] = [S_1]_0 e^{-\Gamma t}$ where S_1 is the concentration of excited state molecules at time t, $[S_1]_0$ is the initial concentration and Γ is the decay rate or the inverse of the fluorescence lifetime. This is an instance of exponential decay. Various radiative and non-radiative processes can de-populate the excited state. In such case the total decay rate is the sum over all rates:

$$\Gamma_{\text{tot}} = \Gamma_{\text{rad}} + \Gamma_{\text{nrad}}$$

where Γ_{tot} is the total decay rate, Γ_{rad} the radiative decay rate and Γ_{nrad} the non-radiative decay rate. It is similar to a first-order chemical reaction in which the first-order rate constant is the sum of all of the rates (a parallel kinetic model). If the rate of spontaneous emission or any of the other rates is fast, the lifetime is short.

1.1.2. Phosphorescence

It is a specific type of photoluminescence related to fluorescence. Unlike fluorescence, a phosphorescent material does not immediately re-emit the radiation it absorbs. The slower time scales of the re-emission are associated with "forbidden" energy state transitions in quantum mechanics. As these transitions occur very slowly in certain materials, absorbed radiation may be re-emitted at a lower intensity for up to several hours after the original excitation. In Phosphorescence a molecule in the excited triplet state may not always use intersystem crossing to return to the ground state. It could lose energy by emission of a photon. A triplet/singlet transition is much less probable than a singlet/singlet transition. The lifetime of the excited triplet state can be up to 10 s, in comparison with 10^{-5} s to 10^{-8} s average lifetime of an excited singlet state. Emission from triplet/singlet transitions can continue after initial irradiation. Internal conversion and other radiation less transfers of energy compete so successfully with phosphorescence that it is usually seen only at low temperatures or in highly viscous media. This may occur after fluorescence. The energy from some shifting electrons (caused by exposure to shortwave and/or long wave ultraviolet lamps) can be "stored" within the material and be released at a later time. If the energy release is delayed for a period of seconds, minutes, hours, or days, it is known as phosphorescence. Or, a mineral which continues to glow for an interval after the ultraviolet light source has been turned off. Commonly seen examples of phosphorescent materials are the glow-in-the-dark toys, paint, and clock dials that glow for some time after being charged with a bright light such as in any normal reading or room light. Typically the glowing then slowly fades out within minutes (or up to a few hours) in a dark room.

1.1.2.1. Intra-molecular redistribution of energy between possible electronic and vibrational states. The molecule returns to the electronic ground state. The excess energy is converted into vibrational energy (internal conversion), and so the molecule is placed in an extremely high vibrational level of the electronic ground state. This excess vibrational energy is lost by collision with other molecules (vibrational relaxation). The conversion of electronic energy into vibrational energy is helped if the molecule is "loose and floppy", because it can reorient itself in ways which aid the internal transfer of energy.

1.1.2.2. A combination of intra- and inter-molecular energy redistribution. The spin of an excited electron can be reversed, leaving the molecule in an excited triplet state; this is called intersystem crossing. The triplet state is of a lower electronic energy than the excited singlet state. The probability of this happening is increased if the vibrational levels of these two states overlap. For example, the lowest singlet vibrational level can overlap one of the higher vibrational levels of the triplet state. A molecule in a high vibrational level of the excited triplet state can loose energy in collision with solvent molecules, leaving it at the lowest vibrational level of the triplet state. It can then undergo a second intersystem crossing to a high vibrational level of the electronic ground state. Finally, the molecule returns to the lowest vibrational level of the electronic ground state by vibrational relaxation. Main processes of luminescence are (1) absorption of excitation energy and stimulation of the system into an excited state, (2) transformation and transfer of the excitation energy and (3) emission of light and relaxation of the system into an unexcited condition. Different types of luminescence centre include transition metal ions, (Mn^{2+}, Cr^{3+}, Fe^{3+}), rare earth elements ($RE^{2+}/^{3+}$), actinides (uranyl UO^{22+}), heavy metals (Pb^{2+}, Tl^{+}), electron–hole centre's (S^{2-}, O^{2-}, F^{-} centre's), more extended defects (dislocations, clusters).

1.1.3. Luminescence in transition metal ions

Transition metal is an element whose atom has an incomplete *d* sub-shell, or which can give rise to cations with an incomplete *d* sub-shell. The electronic structure of transition metal atoms can be written as $[ns^2(n-1)d^m]$, where the inner *d* orbital has more energy than the valence-shell *s* orbital. In divalent and trivalent ions of the transition metals, the situation is reversed such that the *s* electrons have higher energy. Consequently, an ion such as Fe^{2+} has no *s* electrons: it has the electronic configuration $[Ar]3d^6$ as compared with the configuration of the atom, $[Ar]4s^2 3d^6$, zinc, cadmium, and mercury are not classified as transition metals [7] as they have the electronic configuration $[d^{10}s^2]$, with no incomplete *d* shell. A characteristic of transition metals is that they exhibit two or more oxidation states, usually differing by one. As implied by the name, all transition metals are metals and conductors of electricity. Transition metal compounds are paramagnetic when they have one or more unpaired *d* electrons [8].

In general transition metals possess high density, high melting points and boiling points are due to metallic bonding by delocalized d electrons, leading to cohesion which increases with the number of shared electrons. However the group 12 metals have much lower melting and boiling points since their full *d* sub-shells prevent *d*–*d* bonding. There are a number of properties shared by the transition elements that are not found in other elements, due to partially filled *d* shell, which include (i) the formation of compounds whose color is due to *d*–*d* electronic transitions, and (ii) the formation of compounds in many oxidation states, due to the relatively low reactivity of unpaired *d* electrons [9].

(i) *Charge transfer transitions*: An electron may jump from a predominantly ligand orbital to a predominantly metal orbital, giving rise to a ligand-to-metal charge-transfer (LMCT) transition. These can most easily occur when the metal is in a high oxidation state. For example, the color of chromate, dichromate and permanganate ions, mercuric iodide, HgI_2, is red that is due to LMCT transitions. As this example shows, charge transfer transitions are not restricted to transition metals [10] a metal-to ligand charge transfer (MLCT) transition will be most likely when the metal is in a low oxidation state and the ligand is easily reduced.

(ii) *d–d transitions*: In complexes of the transition metals the *d* orbitals do not all have the same energy. The pattern of splitting of the *d* orbitals can be calculated using crystal field theory. The extent of the splitting depends on the particular metal, its oxidation state and the nature of the ligands. In this case, an electron jumps from one *d*-orbital to another.

1.1.4. Luminescence in rare earth metal complexes

Considerable improvement in the field of luminescent materials has been made by the introduction of rare earth ions as luminescent species. An important breakthrough was the use of Eu^{3+} activated materials as the red component for color-television screens. A couple of years later the use of rare earth activated phosphors yielded considerable improvements in luminescent lamps and X-ray intensifying screens. Even more recently Philips introduced the energy-saving SL lamps. Trivalent rare earth (RE) complexes, which featured line-like emissions, high luminescent efficiency, high quantum efficiency and easy synthesis, have been introduced as the emission material into the field of organic light-emitting diodes (OLEDs) [11–14].

Rare earths are a family of 17 elements with atomic number 21, 39 and 57–71. Out of these, the element with atomic number 57, lanthanum has no free electron in the 4*f* shell, while with atomic number 71; lutetium has a completely filled 4*f* shell with 14 electrons. One peculiar nature of all 13 elements among the rare earths, starting from cerium to ytterbium, is that the 4*f* shell is incompletely filled, but is completely screened by the outer 5*s* and 5*p* sub shells, which are completely filled. The optical and electromagnetic properties of these 13 rare earth elements are essentially due to the screening of this incompletely filled 4*f* shell. Luminescence in tri positive RE ions arises mainly due to energy level transition within the 4*f* shell, which is generally forbidden by quantum mechanical spin and parity prohibition rules. Efficient luminescence can still occur in these ions under conditions where such ions do not occupy a position having a centre of symmetry in a crystalline lattice. Some of the tri positive ions such as europium, terbium and dysprosium are good luminescent emitters-a factor depending on the number of electrons in its 4*f* shell. The ions, which are inert to luminescent emission, are those of yttrium, lanthanum, gadolinium and lutetium.

It is well established that rare earth metal chelates are characterized by highly efficient intra-energy conversion from the ligand singlet (S_1) into the triplet (T_1), hence to the excited state of the central rare earth metal ion [15,16]. The metal ions exhibit sharp spectral bands corresponding to $^5D_x \rightarrow {}^7F_x$ transitions. This mechanism is characterized by high (20–95%) photoluminescence efficiency for the molecules suspended in dilute solution [17,18]. Unlike common fluorescent and phosphorescent compounds, rare earth complexes exhibit high luminescence efficiency with sharp spectral bands involving electrons associated with inner 4*f* orbitals of the central rare earth metal ions.

Incorporation of lanthanide complexes in the emitting layer of OLEDs offers two main advantages: (i) improved color saturation and (ii) higher efficiency of the OLED. Because of the sharp emission bands of the trivalent lanthanide ions (with a full-width at half maximum of less than 10 nm), lanthanide luminescence is highly monochromatic. This results in a much better color saturation than when organic molecules are used as the emissive material. In this case the band widths of the emission bands are typically around 80–100 nm. A saturated monochromatic emission is necessary for the development of full-color displays based on OLEDs. Broad emission bands will give dull colors. The efficiency of OLEDS is limited to 25% by spin statistics. However, when lanthanide complexes are used, the efficiency is not limited because the excitation energy can be transferred both from an excited singlet or triplet to the lanthanide ion. Although one often predicts a bright future for lanthanide-doped OLEDs, it has been learned from practice that the use of lanthanide complexes in OLEDs generates several problems.

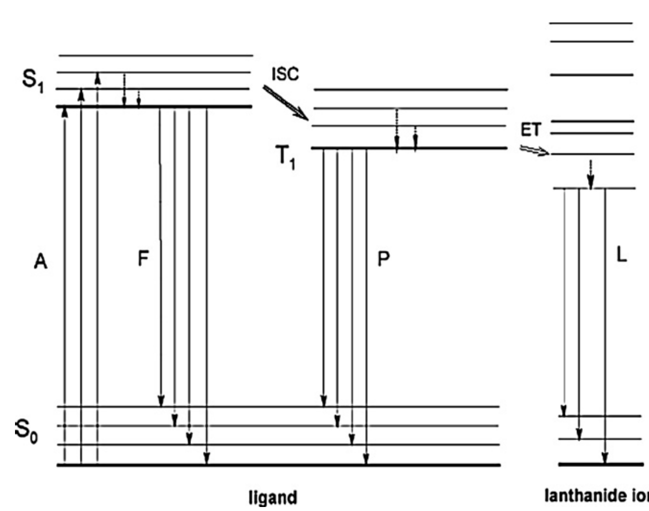


Fig. 1. Photo physical processes in lanthanide β-diketonate complexes. Where A = absorption; F = fluorescence; P = phosphorescence; L = lanthanide centered luminescence; ISC = inter system crossing; ET = energy transfer.

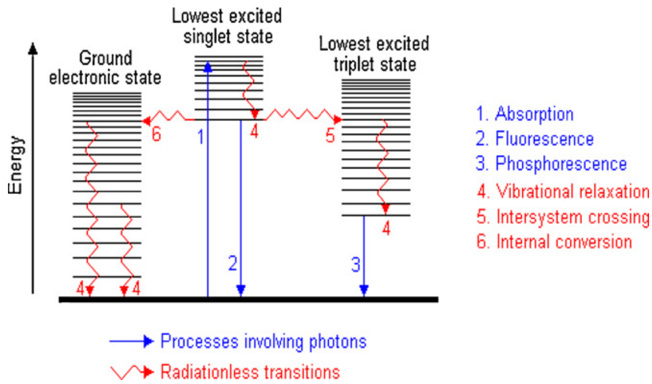


Fig. 2. Possible physical process following absorption of a photon by a molecule.

One difficulty is the poor film-forming properties of low-molecular weight lanthanide coordination compounds. Other problems are the low electroluminescence efficiency (due to poor charge-carrier transporting properties), and the bad long-term stability of the rare earth complexes.

Y(III), La(III) and Tb(III) predominantly play a key role to enhance the luminescence in micelle solution and proved that an efficient and brighter luminescence and economical complexes can be obtained by selection of proper ligand and introduction of another metal ion into the complexes [19]. The photo physical process in lanthanide β-diketonate complexes leading to lanthanide centered luminescence and the possible physical process following absorption of a photon by a molecule are shown in Figs. 1 and 2, respectively.

Absorption of electrons takes place in singlet states, i.e., from S_0 state to S_1 state of the ligand, and reaches to T1 through inter system crossing (ISC). A part of it comes to the ground state S_0 of the ligand. While crossing, the remaining energy is transferred to the lanthanide ion, leading to luminescence [20]. This is also known as antenna effect.

1.1.5. Luminescence in actinides

The actinide series encompasses the 15 chemical elements with atomic numbers from 89 to 103, actinium to lawrencium The actinides are usually considered to be *f*-block elements; they show much more variable valence than the lanthanides. All actinides are radioactive and release energy upon radioactive decay; uranium, thorium, and plutonium, the most abundant actinides on Earth within actinides, there are two overlapping groups: transuranium elements, which follow uranium in the periodic table and transplutonium which follow plutonium. The most abundant or easy to synthesize actinides are uranium and thorium, followed by plutonium, americium, actinium, protactinium and neptunium. Actinides have similar properties to lanthanides. The 6*d* and 7*s* electronic shells are completed in actinium and thorium, and the 5*f* shell is being filled with further increase in atomic number; the 4*f* shell is filled in the lanthanides. The characteristics of emission spectra are often very sensitive to the energetic position of these states. Even more drastic is their influence on the temperature quenching of these emissions. Direct feeding of the 5^D levels of Eu^{3+} by charge-transfer states occurs, but the reverse process is also possible. The spectral position of transitions to charge-transfer and $f^{n-1}d$ states can influence energy transfer probabilities. Metal ion-metal ion charge transfer states are also of great importance in this field. Some hexavalent uranium exhibits luminescence properties. This emission is due to an octahedral UO_6^{6-} group and not to the well-known uranyl (UO_2^{2+}) group. Charge-transfer states involving 5*f* and possibly 6*d* levels determine the dependence of the emission characteristics on the host lattice.

1.1.6. Luminescence in heavy metals

A heavy metal is a member of a loosely defined subset of elements that exhibit metallic properties. It mainly includes the transition metals, some metalloids, lanthanides, and actinides. Luminescence detection of transition and heavy metals by inversion of excited states, synthesis, spectroscopy, and X-ray crystallography of Ca, Mn, Pb, and Zn complexes of 1,8-anthraquinone-18-crown-5 was carried out by Kadarkaraisamy and Sykes [21]. They achieved optimum fluorescence enhancement using cations of high charge, large cations that form long bonds within the host, and cations which do not coordinate solvent or the counter anion, all of which are necessary for inversion of excited states to occur.

1.1.7. Luminescence in electron–hole centers

This method makes use of electrons trapped between the valence and conduction bands in the crystalline structure of certain types of matter such as quartz, feldspar, and aluminum oxide. The trapping sites are imperfections of the lattice impurities or defects. The ionizing radiation produces electron-hole pairs, electrons are in the conduction band and holes in the valence band. The electrons which have been excited to the conduction band may become entrapped in the electron or hole traps. Under stimulation of light the electrons may free themselves from the trap and get into the conduction band. From the conduction band they may recombine with holes trapped in hole traps. Emission of light occurs if the centre with the hole is a luminescence centre (radiative recombination centre).

1.1.8. Luminescence extended defects

Extended defects can also generate luminescence. Lee and Choi [22] studied the temperature and power dependence of the photoluminescence spectra which arose from the dislocations at the hetero-interface of very thin and partially strained $Si_{0.6}Ge_{0.4}$ alloys grown on silicon substrates.

2. Evolution of OLEDs

Prior to the OLEDs, many display technologies such as cathode ray tube, inorganic light emitting diodes, liquid crystal displays, plasma displays were leading in the display market. All these displays have their own limitations including bulkiness, low viewing angle, color tunability, etc. The essential requirements of present generation displays are reproduction of good light quality, brightness, contrast, improved color variation, high resolution, low weight, reduction in thickness, reduction in cost, low power consumption. All these short comings are rectified in these OLED devices and a new flat panel display technology [23] on these organic based devices commonly known as OLEDs emerged.

Key advantages of these OLEDs are that the displays are flat, lighter in weight, emissive fast, operate at a very low voltage and offer the prospect of simple fabrication. They have excellent viewing angle and the potential of much low power consumption than backlit liquid crystal displays.

2.1. Structure of OLED

Structure of different OLEDs is shown in Fig. 3. A single-layer OLED is made of a single organic layer sandwiched between the cathode and the anode. This layer must not only possess high quantum efficiency for photoluminescence, but the layer must also have good hole and electron transport properties. In a two-layer OLED, one organic layer is specifically chosen to transport holes and the other layer is chosen to transport electrons. Recombination of the hole–electron pair takes place at the interface between the two layers, which generates electroluminescence. In a three-layer OLED an

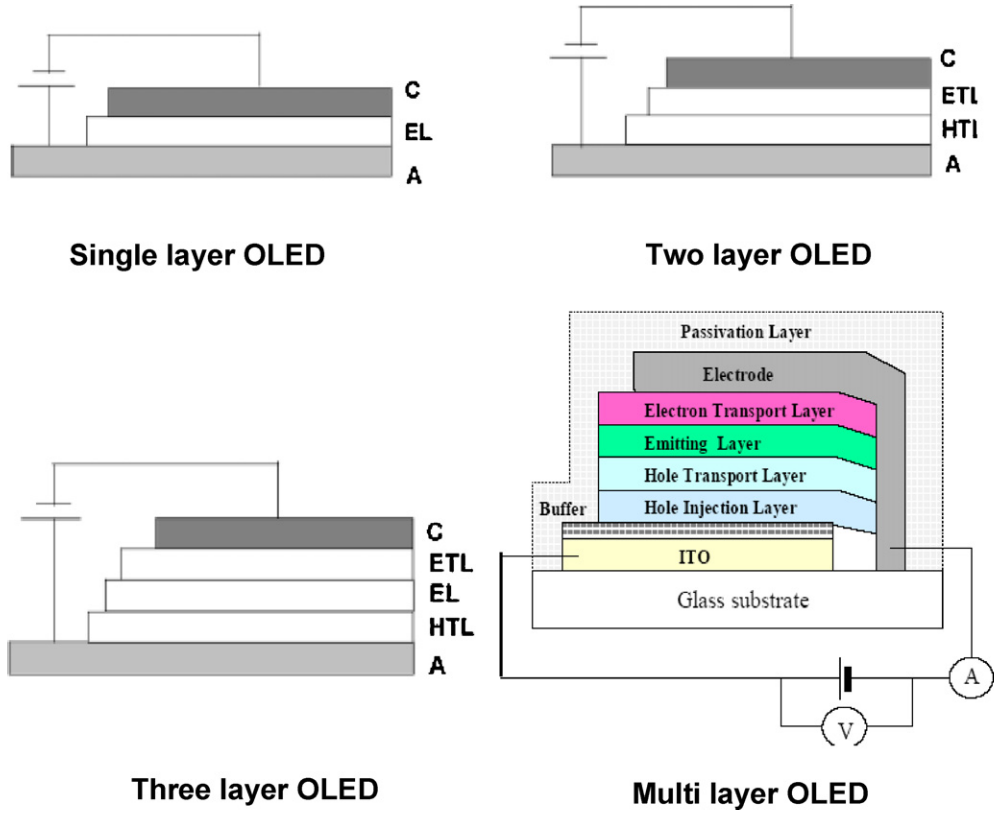


Fig. 3. Structure of different OLEDs. Where C = cathode (typically aluminum); EL = emitting layer; ETL = electron transport layer; HTL = hole transport layer; HIL = hole injection layer; A = anode small molecules.

additional layer is placed between the hole transporting layer and the electron-transporting layer. The emitting layer is primarily the site of hole–electron recombination and thus for electroluminescence. This cell structure is useful for emissive materials that do not possess high carrier transport properties. In a multi-layer OLED an electron injection layer is also included. Introduction of multi-layer device structure eliminates the charge carrier leakage as well as exciton quenching, as excited states are generally quenched at the interface of the organic layer and the metal. Multi layer OLEDs consist of different layers namely ITO glass plate, hole injection layer (HIL), hole transport layer (HTL), emitting layer (EML), electron transporting layer (ETL) and anode.

Substrate: This is usually clear plastic, glass, or metal foil, which is a transparent and conductive substrate with high work function ($\varphi_W \approx 4.7$–4.9 eV).
Anode: This is as a transparent electrode to inject holes into organic layers. Important requirement of this layer is that it must have low roughness and with high work function.
Hole injection layer (*HIL*): The materials with high mobility, electron blocking capacity and high glass transition temperature can be used as HIL.
Hole transport layer (*HTL*): Hole transporting layer plays an important role in transporting holes and blocking electrons, thus preventing electrons from reaching the opposite electrode without recombining with holes.
Emissive layer (*EML*): The layer in between HTL and ETL is a good emitter of visible photons, generally known as emissive layer (EML). This layer can be a material made of organic molecules or polymers with high efficiency, lifetime and color purity.
Electron transport layer (*ETL*): This layer should have good electron transporting and hole blocking properties.

Table 1
Materials generally used in different layers of OLED's.

Layer of OLED's	Materials generally used in different layers of OLED's
Anode	High work function; ITO, IZO, ZNO; TCP (PANI, PEDOT); Au, Pt, Ni, p-Si; ITO; Surface treatment; Plasma (O_2, NH_3); Solution (Aquaregia); Thin insulator AlO_x, SiO_x; RuO_x (4.9 eV); MoO_x (5.4 eV)
Cathode	Low work function; Mg:Ag; Li:Al; Ca. . .; thin insulator; LiF; MgO_x.
HIL	HOMO level; Spiro-TAD; CuPc; m-MTDATA; PTCDA; 2TNATA; TPD; NPD; DPVBi, . . .; PPV; PVK; Dendrimer
ETL	LUMO level; Alq_3; $Bebq_2$; PBD; OXD; TAZ; BCP
EML: Dopant	Alq_3; CPB; Balq; DPVBi; Rubrene; Spiro DPVBi; Quinacridone; Coumarin; DSA; $Ir(ppy)_3$; Pt(OEP); emitting assistant; rare earth complexes

Cathode: Cathode is typically a low work function metal alloy ($\varphi_W \approx 2.9$–4.0 eV). The cathode injects electrons into emitting layers. It is transparent in top emitting devices. It must be stable to the organic layers under it.

Deposition of all these layers on ITO glass substrate itself is too critical because of the sensitivity of the material to different factors such as high temperature, incorporation of dust during fabrication. Various materials generally used in different layers of OLED are tabulated in Table 1.

2.2. Types of OLEDs

Different formulations of OLEDs namely, passive-matrix OLED (PMOLED), active-matrix OLED (AMOLED), transparent OLED, top-emitting OLED, bottom-emitting OLED, foldable OLED and white OLED along with their characteristics are described in Table 2.

Table 2
Different formulations of OLEDs and their characteristics.

Formulation of OLED's	Structure	Material	Emission type	Power consumption	Cost	Applications	Ref.
PMOLED	Anode/organic layer/cathode	Organic	–	More	Expensive	For small screen and cell phone applications	[24]
AMOLED	Anode/organic layer/cathode with TFT matrix	Organic	Top	Less	Cheaper	Computer monitor, large TV screen applications	[24]
Transparent OLED	Substrate/anode/conductive layer/emission layer/cathode	Organic	From both the sides	–	–	Head up displays	[24]
Top emitting OLED	Substrate/anode/conductive layer/emission layer/cathode	Organic	Top	–	–	–	[24]
Bottom emitting OLED	Transparent glass/TFT/ITO/emission layer/cathode	Organic	Bottom	–	–	Smaller as well as larger displays	[24]
Foldable OLED	–	Polymers	–	Less	Cheaper	Smaller as well as larger displays	[24]
White OLED	–	Conjugated and metal complexes, organic dyes	–	–	–	Back light in OLEDs	[25]

2.3. Materials for OLEDs

Different classes of organic semiconductors used in OLEDs are shown in Fig. 4. OLED materials for displays can be made by the following materials, each of which has its own distinct fabrication process and a different set of advantages and limitations. The color is decided by the band gad of the material. Small molecular material exists usually as crystal. A popular example is Alq_3. Polymer material is usually presents in amorphous state in the device. Popular materials are PPV and MEH-PPV. Two key characteristics of OLEDs based on organic materials are large size and moderate brightness.

2.4. Generation of Light from OLEDs

Meeting predicted that worldwide energy consumption needs over the next hundred years will require fundamental changes in how we generate and use energy. The systems that aim to produce white light for illumination purposes are collectively termed solid-state lighting (SSL). Solid-state devices have recently achieved electrical-to-optical power conversion efficiencies of 76% at infrared wavelengths [26]. Unlike incandescent and fluorescent lightings, for which indirect processes (electricity to heat, electricity to gas discharges) limit efficiencies, there is no known fundamental physical barrier to SSL achieving similar (or even higher) efficiencies for bright white light. Even if "only" 50% efficient SSL were to be achieved and displaced current white-lighting technologies completely, the impact would be enormous. The electricity used for lighting would be cut by 62%, and total electrical energy consumption would decrease by roughly 13%. The savings in energy production that could be enabled by SSL would also have an important impact on the environment. If we can simultaneously achieve long device lifetimes and high energy efficiency in devices by addressing the scientific challenges, SSL based on OLEDs could become a formidable economic force and the greatest technological achievement in the field of lighting.

Light generated by the organic emissive region of OLEDs can be emitted in (i) external modes, which can escape through the substrate in the forward viewing direction, (ii) substrate-wave guiding modes, which extend from the substrate/air interface to the metal cathode; and (iii) organic-wave guiding modes, which are confined within the high-refractive-index organic layers. The conventional planar-type OLEDs allow approximately 20% of all the light emission generated in an OLED to escape through the external modes, creating a very low light extraction efficiency of 20% Various optical designs have been patented and/or reported, which may increase the light extraction efficiency to 30–40%, corresponding to a 50–100% increase. This technology incorporates a novel optical design to efficiently extract all wave guiding modes in an OLED, and can potentially lead to light extraction efficiencies up to 80%. The fabrication of this light extraction enhancement mechanism is compatible with existing high throughput, low-cost printing technologies, and will not noticeably change the electrical performance of the original OLED device. Unlike many existing methods, this technology will not change the emission spectrum, nor will it significantly alter the angular emission pattern. Therefore it can easily be incorporated into existing full-color displays or white-light-emitting devices without modifying the driving electronics. Resolution as good as 20 μm can be achieved by making this technology suitable for monochromatic or full-color displays.

Quality of light generated by OLEDs can be evaluated from three parameters namely Commission Internationale de L'Eclairage (CIE) coordinates, color rendering index (CRI), and correlated color temperature (CCT). The emitting light color of a lighting source can be characterized by the CIE coordinates, which describe how the human eyes perceive the emission color of any light source (with an arbitrary emission spectrum) with a pair of two numbers [x, y] in 1931 CIE chromaticity diagram.

2.5. Light emitting mechanism from OLED device

Multi layer OLED device have several layers, which differ in their properties. When voltage is applied across the OLED, current flows through the device. Thus, the cathode gives electrons to the emissive layer and holes are injected from the anode, forming exciton pairs in the emissive layer. When the charges in exciton pairs are combined, they give rise to light emission. The color of the light depends on the type of organic molecule in the emissive layer. Emission color is basically determined by the energy difference of HOMO and LUMO of the emitting organic material. The intensity or brightness of the light depends on the amount of electrical current applied. Consequently by changing these active materials the emission color can be varied across the entire visible spectrum. Light emitting mechanism from an OLED device is shown in Fig. 5.

Large amount of light emitted from a light emitting diode (LED) being trapped inside the semiconductor structure is the consequence of the large value of the refractive index. The total internal reflection is the major factor responsible for the small light extraction efficiency, while the other important contributions to the losses include the internal absorption and blocking of the light by contacts. Assessment of intensity of light sources using one of

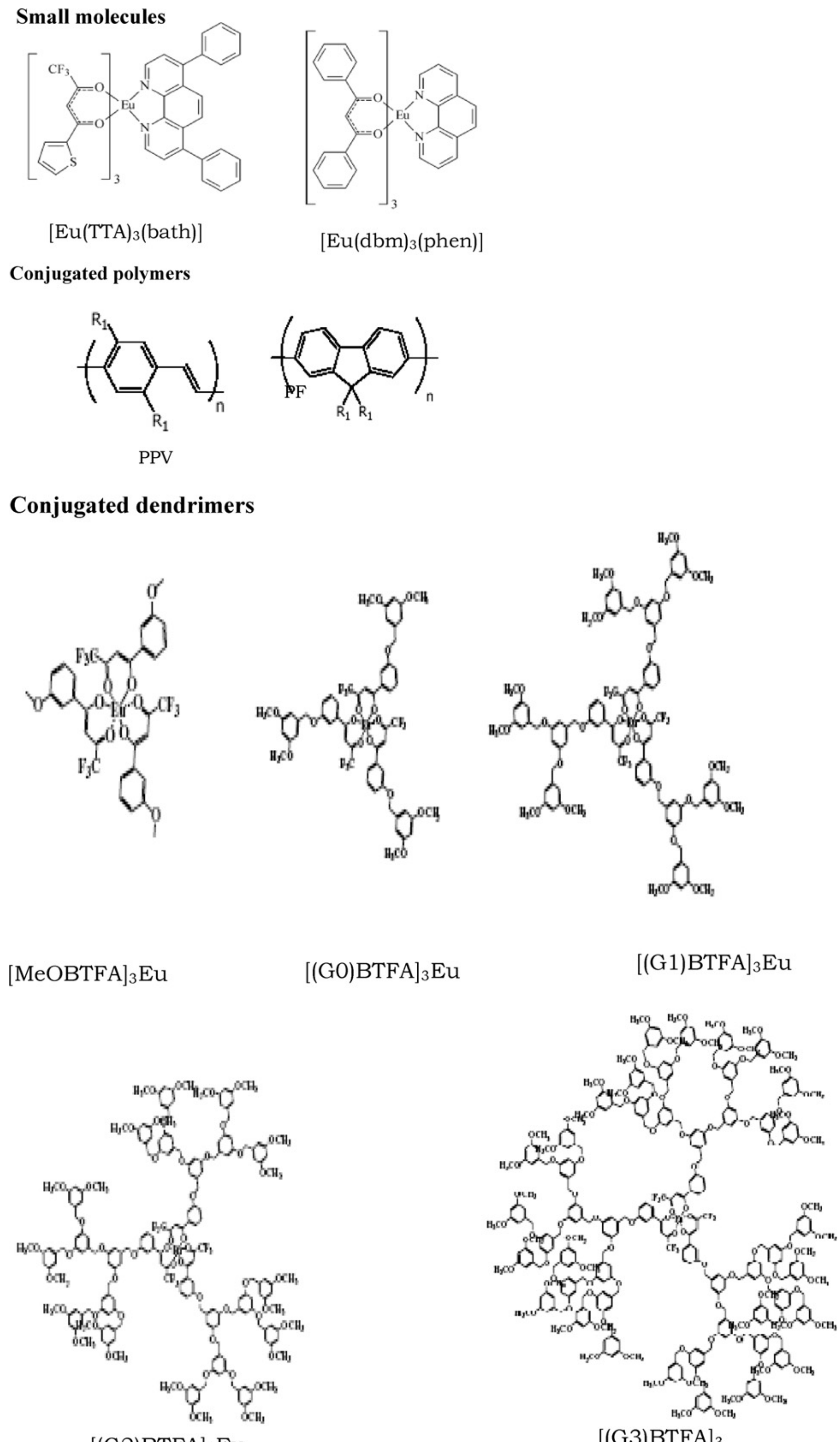


Fig. 4. Different classes of organic semiconductors used in OLEDs. Where TTA is 2-thenoyl trifluoro acetone, bath is batho phenanthroline and dbm is dibenzoyl methane, Phen is 1,10-phenanthroline, PPV is poly-phenylene vinylene, PF is poly-fluorene and BTFA is benzoyl trifluoroacetone.

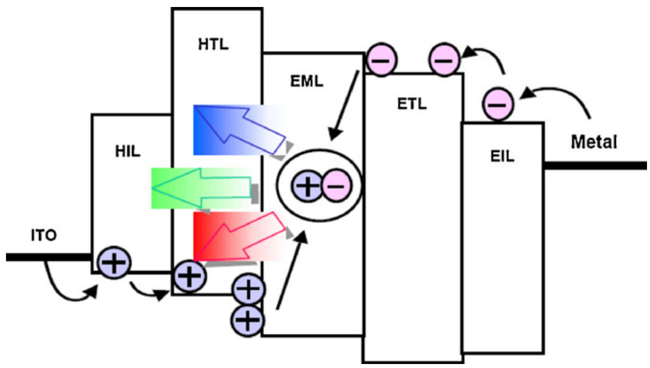


Fig. 5. Light emitting mechanism from an OLED device.

the following techniques: (i) radiometry and (ii) photometry [27]. Zhmakin [28] reported a way for the enhancement of light extraction from light emitting diodes.

3. OLED core fabrication technologies

OLED devices/displays can be fabricated in two ways namely vacuum deposition technique and solution techniques including spin coat technique, ink jet technique, casting, etc.

Vacuum deposition is the widely used technique, but it is time consuming as high vacuum state is to be obtained and is difficult to deposit over large area. Lanthanide-based OLEDs are prepared by vacuum deposition of the different layers (hole injection layer, emitting layer, electron transport layer, cathode) on the ITO substrate. This technique is applicable only for volatile and thermally stable lanthanide complexes. Unfortunately, most volatile lanthanide β-diketonate complexes are not the ones with the best luminescence properties. Many β-diketonate complexes cannot be sublimed without considerable thermal decomposition, or give deposited layers of an inferior quality. The films of lanthanide β-diketonate produced by vacuum deposition have poor charge-carrier properties. Especially the transport of electrons is problematic. Because of the unbalanced injection and transport of charge carriers, recombination often takes place at sites other than the emitting layer. This not only leads to low electroluminescence efficiency, but also to a reduced life time of the OLED. This approach involves the vacuum batch deposition of small-molecule organic material layers onto a glass or silicon backplane. The technology is well proven but currently only suits mass-production of small or medium-sized displays up to about 15 in. in diameter. The fabrication of larger displays is hindered by the performance of the shadow masks that are used to define (pattern) the pixels of the display.

In contrast solution techniques have currently gained momentum as they consume less time easy to deposit thin layer thin film can be deposited over a large area. However, interest in developing PLEDs is rapidly growing, since the manufacturing technologies are solution based ∼ink-jet printing, spin coating, etc., and therefore much cheaper than traditional evaporation techniques are used for OLEDs. The big advantage of polymer light-emitting materials (PLEDs) is that they are soluble and can be deposited onto a glass or flexible plastic substrate under ambient conditions. Polymer technology enables the fabrication of larger screen sizes than small-molecule OLEDs, as there is no need for the shadow masks required by vacuum deposition processing. PLED displays also operate at a lower voltage and are more power-efficient than those based on small molecules.

Besides vacuum deposition technology, solution process can also be employed to prepare EMLs of WOLEDs. Compared with vacuum deposition, solution process offers several advantages as follows: straightforward fabrication procedure, large area coverage, low power consumption, screen printing and ink-jet deposition, etc. For all-phosphorescent WOLEDs, another bonus associated with solution process is the ease of precisely controlling the doping level for every phosphor, especially for preparing multi doped EMLs. However, WOLEDs with solution-processed EMLs are from phosphorescent emitters that can be set into different layers individually to make WOLEDs with multi-EML configuration. Despite the complexity in device fabrication, WOLEDs with multi-EMLs would serve as a good platform with wider scope for device optimization.

The process of fabricating an OLED device/displays passes through several manufacturing steps as follows:

1) *Substrate fabrication*: The first step is the production of the substrate, also known as the backplane. During this stage, thin-film transistor circuits that drive each pixel are placed onto a glass or silicon substrate. The deposition and patterning take place in a clean room and are similar to that used to make integrated circuits. The substrates may be made from plastic also.
2) *OLED deposition*: The next step is the fabrication of the OLED part of the display. This involves the deposition of the active light-emitting layers by either vacuum or wet process deposition techniques, depending on the type of OLED material. Finally, the cathode electrode is deposited by a vacuum or sputtering process.
3) *Encapsulation*: To protect the electronics and active OLED layer from exposure to water vapor and oxygen, these parts are hermetically sealed in a protective package. This is essential to maximize the display's performance and lifetime.
4) *Assembly*: Finally, all parts of the display are assembled to create a complete module.

4. Review on OLED materials/devices

Organic light emitting materials have been attracting attention of researchers from industry and academic institutions owing to their applications in OLEDs [29]. Organic rare earth metal complexes have been potential candidates as emitting materials due to extremely narrow emission line and high internal quantum efficiencies. Many organic complexes were synthesized and used as emitting materials in the OLED with different emission color, such as 1 AZM-HEX is used as a blue emitter, europium as red emitter, Alq_3 and Tb^{3+} complex as green light emitter [30].

The review on organic rare earth complexes in the present investigation mainly encompasses on the following areas, which includes

i) Organic complexes.
ii) Rare earths β-diketonates.
iii) Enhancement of PL spectra in organic complexes and micelle solution.
iv) Organic luminescent complexes in polymer resins.

4.1. Organic complexes

Research in the field of organic complexes started in the year 1904 with the synthesis of β-diketonates, their hydrates and hydroxo bis (β-diketonate) have been synthesized by Blitz [31], Jantzch and Meyer [32] and Van Uitert and Soden [33], respectively. Later in 1959, Moeller and Horwitz demonstrated lanthanide complexes containing nitrogen donor groups [34].

Electroluminescent devices based on anthracene crystals [35] have been demonstrated in the early 1960s. In 1961 Brock et al. suggested that conjugated organic molecules in a host crystal may

be attractive for lasers and masers [36]. Electroluminescence in organic materials was first reported in 1963 by Lampicki and Samelson [37]. Hart and Laming reported a new 1,10-phenanthroline chelates [38]. Interest in rare earth based phosphors began with the discovery of europium activated vanadate by Levine and Palilla in 1964 for color TV picture tubes [39]. Eu(III) tris (β-diketonates) complexes with monocyclic nitrogen donors like pyridine or piperidine had been described by Ohlmann and Charles [40]. In the same year, Melby et al. extended the area of rare earth coordination chemistry and accordingly prepared a variety of new crystalline complexes but their particular interest was on anionic tetra bis(β-diketone) derivatives, which are believed to have eight coordination numbers [41].

In 1969, Dresner for the first time considered organic material for fabrication of practical electroluminescent (EL) device [42]. Gold in 1971 [43] and Drexhage [44] in 1977 prepared large number of organic material having high fluorescence quantum efficiency in the visible spectrum. Organic thin film for EL studies was reported by Kampas and Gouterman [45] in 1977. Bryant and Krier used Eu(III) activated complexes as dopants in inorganic thin film EL devices [46] Kalinowski et al. [47] in 1985 used organic thin films for multicolor display applications. Due to less stability factor of thin film organic EL work was not successful. Interest in undoped organic semiconductors, both small molecules and polymers revived at the end of 1980s as a result of (i) the demonstration of high performance EL devices made of multi layers of vacuum sublimed film of organic material Alq_3, as emitting layer at Eastman Kodak, (ii) the report of field effect transistors made from poly-thiophen [48] and from small conjugated oligomers [49] and (iii) the discovery of EL from conjugated polymer based diodes at Cambridge university [50].

In 1990, Brittain [51] observed that Tb(III) ions were used as a sensitized ions in Eu(III)–Tb(III) aromatic carboxylic acid complexes, but received little attention as far as the fluorescence enhancement of Eu(III) or Tb(III) by Ln(III) ions with the inert 4*f* levels [52] are concerned and further studied fluorescence enhancement in Eu(III) fluorescence by Y(III), La(III) and Gd(III), and discussed the intermediate role of Ln(III) ions in the enhancement of Eu(III) or Tb(III) fluorescence in their complexes and studied in micelle solution [53].

Kido et al. in 1991 investigated the suitability of Eu(III) complex, $Eu(ttfa)_3$, as a red-light emitter, and commonly used as a red phosphors in CRT [11]. In 1993, Kido et al. [54] reported organic electroluminescent devices using lanthanide complexes such as $Tb(acac)_3$ and $Eu(ttfa)_3$. In 1993 Li et al. investigated fluorescence enhancement of Eu(III)–(thenoyl trifluoroacetone)–phenanthroline in micelle solution and Tb(III)–benzoic acid in ethanol solution by adding other Ln(III) (Ln = Y, La, Gd, Lu) ions. From fluorescence excitation, emission and lifetime measurements, they found that the enhancement of Eu(III) luminescence is due to energy transfer from Ln(III) complex to Eu(III) ion and the wrapping effect of the Ln(III) complexes on the Eu(III) complex. Also, it was shown that the enhanced Tb(III) luminescence is only attributed to energy transfer from Ln(III) complexes to Tb(III) complex [55].

In 1995 Takeshi Sano developed novel europium complexes for luminescent devices with sharp red emission which exhibit intense fluorescence at 610 nm with sharp spectral band width [56].

In 1997, Rodriguez-Ubis et al. discovered a simple ligand based on acetophenone bearing excellent quantum yield for the excitation of Eu^{3+} and Tb^{3+} [57]. Tetra-acid ligand derived from acetophenone was synthesized and luminescence properties of their chelates with Eu(III) and Tb(III) were evaluated in aqueous and methanol solutions. These complexes have excellent quantum yields of triplet sensitization of lanthanide luminescence. Uekawa et al. [58] studied PL excitation of Eu complexes with different ligands such as TTA: thenoyl trifluoroacetone, FIHA: 1-(2-fluorenyl)-4,4,5,5,6,6,6-heptafluoro-1,3, hexanedione and DNM: Di (2-naphthoyl) methane and the PL spectrum of TPD (N,N′-biphenyl-N,N′-(3-methyl phenyl)-1,1′-biphenyl-4,4′-diamine).

In 1998, Wang et al. [59] studied the intermolecular energy transfer from coumarin 120 to rare earth ions (Eu(III), Tb(III)) in silica xerogels via sol–gel technique. The characteristic fluorescence intensities of Eu(III) and Tb(III) ions could be increased by a factor of 35 and 8, respectively, as a result of sensitization of C-120 absorption at about 344 nm. The result shows that no complex species between C-120 and rare earth ion are formed in co-doped xerogels. The sensitized emission of rare earth ions is through the intermolecular resonant exchange interaction. The fluorescence intensities of Eu(III) and Tb(III) ions increase to maximum when the C-120 doping concentration is of 0.1 mol%.

In 1999 Hao et al. studied the luminescence behavior of $Eu(TTA)_3$ doped in sol–gel films [60]. The $Eu(TTA)_3$ doped sol–gel films can be formed by dip-coating of the $EuCl_3$ and TTFA co-doped sol. The luminescence intensity of the $Eu(TTA)_3$ doped sol–gel films was significantly increased with the increase of film thickness. Miyamoto et al. synthesized a Eu(III) β-diketonate complex, $Eu(DBM)_3Phen$[61]. Thin film of $Eu(DBM)_3Phen$ doped with phosphorescent material in OLED showed excellent electroluminescent spectra at room temperature which depends on the host materials, energy transfer from triplet states of the phosphorescent materials to the ligand triplet state of the Eu complex. Fu et al. [62] synthesized and studied the luminescent properties of the ternary europium complexes with ligands thenoyltrifluoroacetone (TTA) and phenanthroline (Phen) incorporated into SiO_2 polymer matrix by a sol gel method. The lifetime of rare earth ion Eu^{3+} in SiO_2/PVB gel matrix doped with $Eu(TTA)_3Phen$ was found to be longer than in pure $Eu(TTA)_3Phen$ powder and solvated $Eu(TTA)_3Phen$ in ethanol solution.

Meng et al. [63] in 2000 developed sol–gel derived luminescent thin films doped with rare earth complexes using a new synthesis method with a two-step hydrolysis process. The luminescence spectra, fluorescence lifetime and thermal stability were investigated. RE ions, which are restrained in a silica matrix, present a longer lifetime and higher thermal stability than that in DMF/PVB films containing the corresponding pure complexes. Zheng et al. [64] synthesized and characterized a new carboxylic acid ligand (o-amino-4-hexadecance-benzoic acid, AHBA) and a corresponding terbium complex ($Tb(AHB)_3$). Zhu et al. prepared a novel polyligand europium β-diketone complex with 1-phenyl-3-methyl-4(4-butyl-benzoyl)-5 pyrazolone (HPMBBP) as ligand [5]. This $Eu(TTA)_2(PMBBP)Phen$ complex exhibited intense PL.

In 2001, Heil et al. demonstrated how $Eu(DBM)_3Phen$ can be effectively integrated and luminescence in an organic electroluminescence layer structure through a simple energy transfer from excited host molecules to the dyes is not possible due to lack of energy overlap [65]. Suitable arrangement of different layers selected with respect to charge transport and HOMO–LOMO positions, especially the insertion of a hole blocking layers, allows the whole radiative recombination processes to be focused on the emitting material leading to the emission of light.

In 2002, Tsaryuk et al. showed that the relative contribution of two types of ligands of $Eu(\beta\text{-diketone})_3Phen$ to the Eu(III) spectra changes with the variation of the relative strength of bonding of these ligands [66]. The contribution of the Phen in Eu(III) excitation increases with the increase of acceptor ability of β-diketone. The participation of β-diketone to cation in the degradation of the excitation energy of Eu(III) was investigated in the molecule.

$Ba_3MgSi_2O_8Eu_{21}$, Mn_{21} shows three emission colors: 442, 505, and 620 nm. The 442 and 505 nm emissions originate from Eu_{21} ions, while the 620 nm emission originates from Mn_{21} ions. The excitation bands of three emission colors are positioned around

375 nm. The red emission of Mn_{21} ions has a long decay time of 750 ms due to persistent energy transfer from oxygen vacancies to Mn_{21} ions, while the blue and green bands of Eu_{21} ions have decay times of 0.32 and 0.64 ms, respectively [67].

In 2005 Eu^{3+} doped Y_2O_3, YOF, La_2O_3, LaOF hollow spheres have been synthesized by a facile template route by Wang et al. [68]. Eu^{3+} was doped into the various host materials to make the hollow sphere red-luminescent.

In 2006 a novel green emitting phosphor, Tb^{3+} doped Ca_2GeO_4 was prepared by Yang et al. [69] for the first time by a solid-state reaction. The phosphor showed prominent luminescence in green due to the magnetic dipole transition of $^5D_4 \rightarrow {}^7F_5$. Photo luminescence measurements indicated that the phosphor exhibited bright green emission at about 541 and 550 nm under UV excitation. In addition, Al^{3+} or Li^+ co-doping enhances the green emission from Ca_2GeO_4:Tb^{3+} by about 18 and 4 times, respectively, under UV excitation. Lee et al. [70] synthesized Eu containing nanoparticles using the ultra-dilute solution method. The size of Eu-containing nanoparticles was 30–150 nm and the nanoparticles were soluble in common organic solvents. A study of the dependence of emission intensities of the Eu-containing nanoparticles on the Eu content showed that the emission intensities increased linearly with increasing europium content, while no significant emission concentration quenching phenomenon was observed at the europium content of 0–9.5 mol%.

In 2007 Całus et al. [71] synthesized methoxy (MO) and carbo ethoxy (CE) di phenyl pirazolo quinoline (DPPQ)-derivatives: 6MO[DPPQ], 6MO1pMO[DPPQ], 6MO13pMO[DPPQ] and 6CE[DPPQ]. The photoemission spectra are recorded in organic solvents of different polarities and found to be highly solvate chromic. 6MO[DPPQ] and 6CE[DPPQ] show broad emission bands shifted to the red with the increase of solvent polarity, whereas the phenyl-methoxy derivatives 6MO1pMO[DPPQ] and 6MO13pMO[DPPQ] exhibit the reverse solvatochromism.

In 2008, for the application in OLEDs, the efficient new red phosphorescent iridium(III) complexes, bis[2,3-diphenyl-4-methyl-quinolinato-C2,N] iridium(III) acetylacetonate [Ir(4-Me-2,3-dpq)$_2$(acac)] and bis[2,3-di(4-methoxy-phenyl)-4-methyl-quinolinato-C_2,N] iridium(III) acetyl acetonate [Ir(4-Me-2,3-dpq(OMe)$_2$)$_2$(acac)] were synthesized [72] from the two-step reactions of $IrCl_3 \cdot xH_2O$ with the corresponding ligand. In the photoluminescence (PL) spectra, Ir(4-Me-2,3-dpq)$_2$(acac) and Ir(4-Me-2,3-dpq(OMe)$_2$)$_2$(acac) exhibited the luminescence peak at 604 and 592 nm, respectively. In 2009 Collins et al. [73] presented a facile method for the novel production of surfactant-stabilized aqueous dispersions of tris(8-hydroxyquinoline) aluminium(III) (Alq_3) nanoparticles. These nanoparticles were spherical, less than 10 nm in mean diameter, and highly fluorescent. They also demonstrated the potential scope of these water-based colloids in sol–gel and electro spinning processes by fabricating photo luminescent silica glasses and polymer nanowires, respectively. The development of aqueous based approaches to stable sols of Alq_3 nanoparticles offers significant scope for the future use and application of this technology as emissive materials.

In 2009 Seo et al. [74] fabricated OLED using the novel red phosphorescent hetero leptic tris cyclo metalated iridium complex, bis(2-phenyl pyridine) iridium (III)[2(5′-methylphenyl)-4-diphenylquinoline] [Ir(ppy)$_2$(dpq–5CH$_3$)], based on 2-phenylpyridine (ppy) and 2(5′-methylphenyl)-4-diphenylquinoline (dpq–5CH$_3$) ligand. Complexes of Eu^{3+} ion and ligands like dibenzoyl methane (DBM) as well as fluoro-and methoxy substituted DBMs have been prepared and characterized by Shukla et al. [75] in the year 2010. Symmetric substitution at both the phenyl groups led to improved luminescence in terms of higher quantum yields of emission and longer life time of the excited state ($^5D_0$) of Eu^{3+} ions. In the same year Nandhikonda et al. [76] synthesized of a new white-light fluorophore and its Photo 84 physical characterization is described. The optimization of excitation wavelengths allows the naphthalimide (NI) dyes to display blue, green or white light emission depending on the excitation wavelength.

Thejo Kalyani et al. [77] in 2010 synthesized europium β-diketonate complexes Eu(TTA)$_3$Phen (TTA: thenoyl trifluoroacetone) and Eu$_x$Re$_{(1-x)}$(TTA)$_3$Phen (where Re = Y, Tb) and studied the optical absorption spectra of organic luminescent complexes in different organic solvents to calculate the energy gap of these solvated complexes. The substantial dependence of the electronic absorption spectra of Eu complexes on the solvent is also reported. A new Eu(III)/Tb(III) binuclear coordination compound with red and yellow emissions in solution and solid-state, respectively, has been prepared by Belian et al. [78] in the year 2010. The homo- and hetero bimetallic Ln(III) complexes were characterized by elemental analysis as well as infra-red, absorption (UV–vis) and emission spectroscopy. These complexes display intense red and green emissions, respectively, in the solid-state at room temperature. A new multifunctional compound, 4,40-di-(1-pyrenyl)-40 0-[2-(9,90-dimethylfluorene)]-tri phenyl amine (DPFA) has been designed, synthesized [79] and applied respectively as host emitter, electron- and hole-transporters in organic light-emitting devices (OLEDs). Synthesis, photophysical properties, and electroluminescence performances of a novel deep-red-emitting iridium complex with single-peaked narrow emission band was reported by Guang [80]. In 2011, Bo Hu et al. reported a theoretical investigation of the white-light emission from a single polymer system with simultaneous blue (polyfluorene as a blue host) and orange (2,1,3-benzothiadiazole (BTD)-based derivative as an orange dopant) emission [81]. Novel yellow phosphorescent iridium complexes Ir(PPOHC)$_3$ and (PPOHC)$_2$Ir(acac) (PPOHC: 3-(5-(4-(pyridin-2-yl)phenyl)-1,3,4-oxadiazol-2-yl)-9-hexyl-9H-carbazole) were synthesized and characterized by Tang et al. [82]

4.2. Rare earths β-diketonates

Rare earth β-diketonates are complexes of β-diketones (1,3-diketones) with rare earth ions. These complexes are most popular and most intensively investigated rare earth coordination compounds. This is partially due to the fact that different β-diketones are commercially available and the synthesis of the corresponding rare earth complexes is relatively easy. However, the main drive for the intense research activity on the rare earth β-diketonates was and is still continuing because of their potential of being used in several applications [83]. The first rare earth β-diketonates have been prepared by Urbain at the end of the 19th century. Using tetrakis acetyl acetonate complex of cerium(IV) and the hydrated tris acetyl acetonate complexes of Ln(III), Gd(III) and Y(III). Overview of the measured radiative lifetime for different europium(III) β-diketonate complexes in the solid-state at room temperature for the emitting state $^5D_0$ is given in Table 3.

In the beginning of the 1960s, these compounds were explored as extractants in solvent–solvent extraction processes. In the middle of the1960s, the rare earth β-diketonates were recognized as potential active compounds for chelate lasers or liquid lasers. The golden years (1970–1985) of the rare earth β-diketonates were the period when these compounds were frequently used as NMR shift reagents. In the 1990s, intense research activity on rare earth β-diketonates started, now triggered by the application of these compounds as electroluminescent materials in OLEDs, as volatile reagents for chemical vapor deposition or as catalysts in organic reactions. Figs. 6–8 show the structures of β-diketones with aliphatic substituent's, structures of β-diketones with aromatic and heterocyclic substituent's, Lewis bases that form adducts with rare earth tris β-diketonates, respectively. The molecules are in the keto

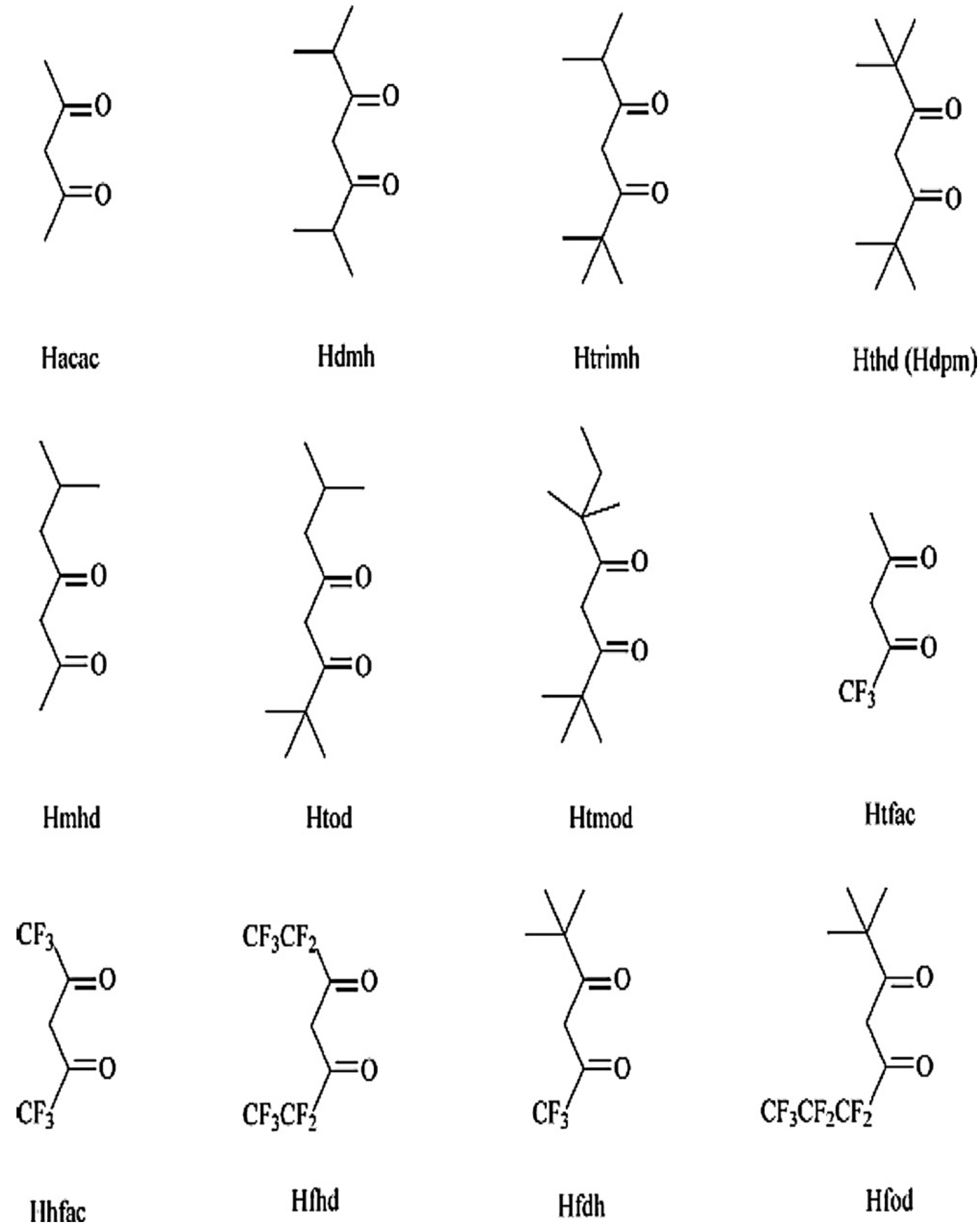


Fig. 6. Structures of β-diketones with aliphatic substituents.

form. *Abbreviations*, name and synonym of all β-diketonates are tabulated in Table 4. Various organic materials were synthesized for red emission in OLED's; some of the organic materials earlier used for red emission and their respective melting and decomposition temperatures are given in Table 5. They are tris complexes of rare earths β-diketonates and adducts with Lewis bases.

4.3. Organic complexes in polymer resins

Fabrication of OLEDs with organic materials by vacuum deposition technique is laborious and cost effective. Hence, shift towards solution processing techniques such as spin coating technique and inkjet technique where we need materials, which have better sticking properties to the substrate and greater mechanical strength. Hence, need arises to dope organic complexes into a polymer, such as polymethylmetacrylate (PMMA), polystyrene, polycarbonates, polyvinylalcohol (PVA), and polyvinyl carbazole (PVK). Another approach of interest is the blending of semiconducting polymers together, where one possesses good hole-transport properties and another possesses good electron-transport properties and provide for a blended ambipolar host for the emissive layer. The polymer blend may be a more challenging approach than the doping of a polymer with small molecules because it can result in materials phenomena, such as vertical phase segregation [123,124], that can decrease device efficiency and lifetime. While blends of conjugated polymers in OLEDs have been widely studied [125] with external quantum efficiencies as high as 6% [126,127].

In 2003, Hu et al. [128] adopted emulsifier-free emulsion polymerization to synthesize rare earth containing submicron polymer particles under microwave irradiation. To control the size and distribution of the particle, the relationship between reaction time, monomer content, and particle radius was studied for the polymerization of methyl methacrylate (MMA) in the absence and presence of rare earth ions, in which water was used as solvent, and potassium per sulfate was used as initiator. For particles containing rare earth ions, characterization shows that mole percentage of Eu(III) ion in the surface layer with a thickness of 5 nm, estimated from X-ray photo electron spectroscopy (XPS), is always larger than

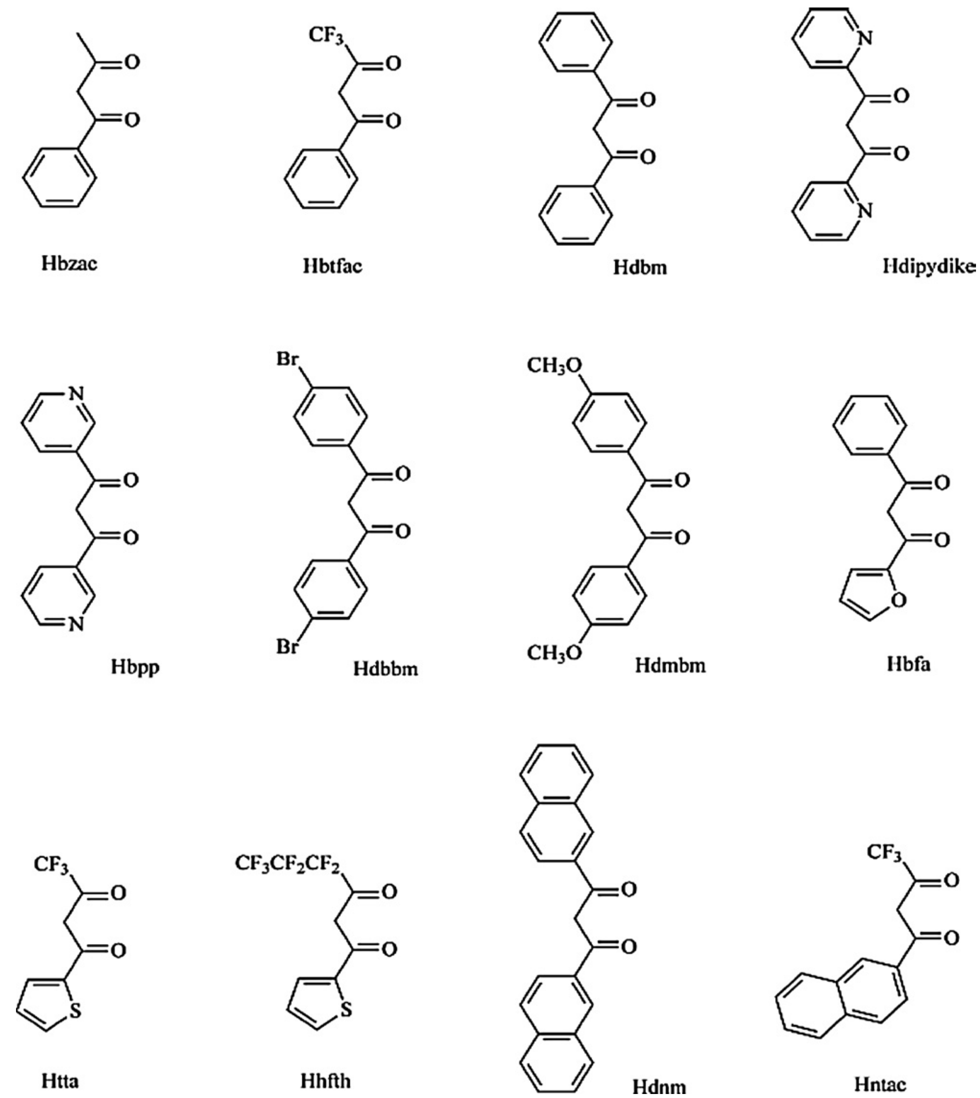


Fig. 7. Structures of β-diketones with aromatic and heterocyclic substituents.

Table 3
Luminescence lifetimes of some Eu(III) β-diketonate complexes.

Compound	Lifetime (ms)	Ref.
[Eu(btfac)$_3$(phenNO)]	0.37	[84]
[Eu(btfac)$_3$(H$_2$O)$_2$]	0.17	[84]
[Eu(tta)$_3$(dbzso)$_2$]	0.71	[85]
[Eu(tta)$_3$(H$_2$O)$_2$]	0.26	[85]
[Eu(btfac)$_3$(H$_2$O)$_2$]	0.32	[86]
[Eu(dmbm)$_3$Phen]	0.34	[87]
[Eu(mdbm)$_3$Phen]	0.37	[87]
[Eu(dbm)$_3$Phen]	0.43	[87]
[Eu(mfa)$_3$Phen]	0.47	[87]
[Eu(bzac)$_3$Phen]	0.61	[87]
[Eu(bzac)$_3$(H$_2$O)$_2$]	0.41	[88]
[Eu(bzac)$_3$Phen]	0.43	[88]
[Eu(bzac)$_3$(phenNO)]	0.46	[88]
[Eu(tta)$_3$(ptso)$_2$]	0.59	[89]
[Eu(tta)$_3$Phen]	0.97	[89]
[Eu(tta)$_3$(dmso)$_2$]	0.72	[90]
[Eu(hfac)$_3$(monoglyme)]	0.93	[91]
[Eu(hfac)$_3$(diglyme)]	0.96	[91]
[Eu(dbm)$_3$Phen]	1.99	[92]

the value estimated by inductively coupled plasma atomic emission spectrometer (ICP-AES) for the whole particle, indicating that surface enrichment of rare earth ions took place during the polymerization.

In 2004, Liu et al. [129] doped europium ternary complexes namely Eu(DBM)3phen, Eu(DBM)$_3$(DB-bpy), Eu(DBM)3(DN-bpy) and Eu(DBM)3biq (DBM, Phen, DB-bpy, DN-bpy and biq refer to Dibenzoylmethane, 1,10-phenanthroline, 4,4-Di-tert-butyl-2,2-dipyridyl, 4,4-Dinonyl-2,2-dipyridyl and 2,2′-Biquinoline, respectively) in PMMA matrix. The luminescence properties of the composites were investigated by emission spectroscopy and lifetime measurements. The composites formed by Eu(III) complexes, Eu(DBM)$_3$Phen, Eu(DBM)$_3$DB-bpy and Eu(DBM)$_3$DN-bpy, exhibit strong luminescence and similar emission spectral characteristics. Whereas, Eu(DBM)$_3$biq shows large differences in its luminescence spectrum compared to those of other complexes. Liu et al. [130] doped europium β-diketonates namely Eu(DBM)$_3$, Eu(BA)$_3$ and Eu(TTA)$_3$ in PMMA matrix. Eu(III) ions in the doped Eu(DBM)$_3$/PMMA systems have two distinct symmetric sites and the emission band changes greatly with the compositions. Eu(III) in the Eu(BA)$_3$/PMMA systems gives only one symmetric site in the doped systems and the emission band changes slightly with the compositions.

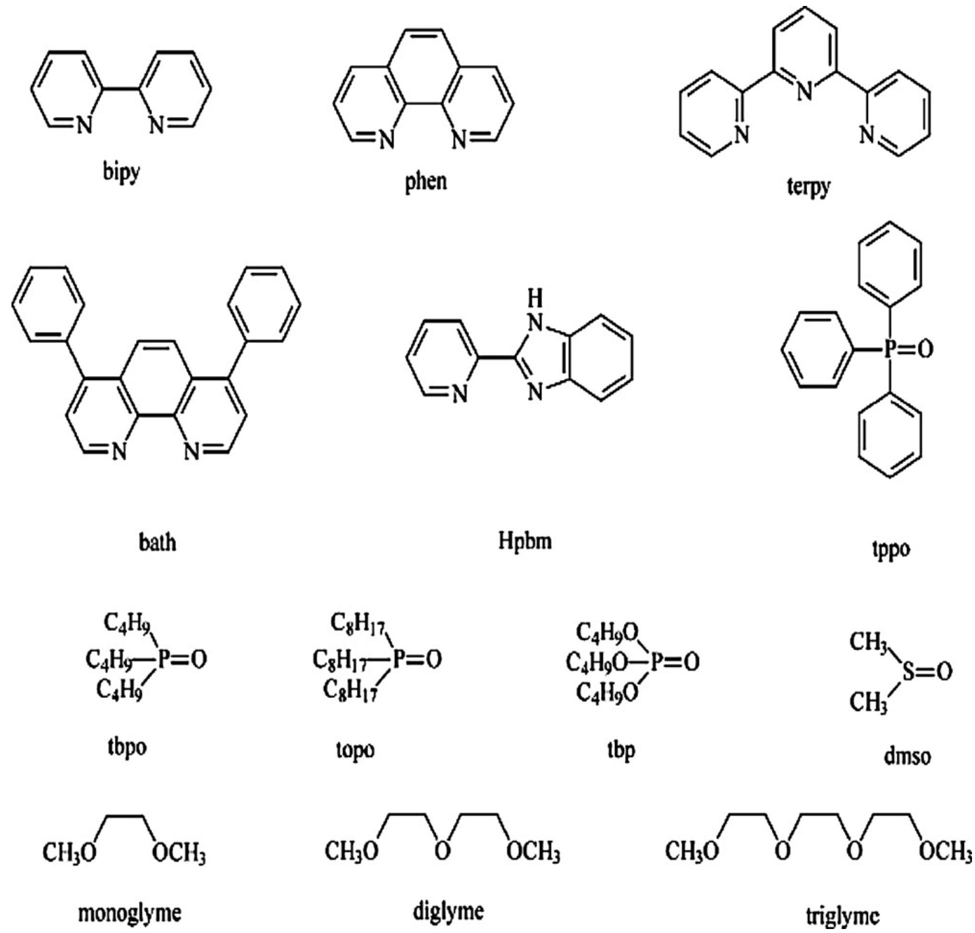


Fig. 8. Lewis bases that form adducts with rare earth tris β-diketonates.

Jiu et al. [131] studied the fluorescence enhancement of $Eu(DBM)_3Phen$ as well as $Tb(DBM)_3Phen$ in PMMA. A combinatorial methodology was adopted to allow rapid optimization of the fluorescence enhancement conditions of thin-film samples in arrays of microwells. Based on $Eu(DBM)_3Phen$ doped PMMA, three material libraries were generated in order to compare the effects of species identity and $Tb(DBM)_3Phen$ content to the effect of other complexes containing enhancing ions (La^{3+}, Gd^{3+}, Dy^{3+}, Y^{3+}, Ce^{3+}) on the luminescence efficiency of the Eu^{3+} complex in PMMA. The fluorescence enhancement of $Eu(DBM)_3Phen$ in PMMA is considered to originate from intra-molecular and intermolecular energy transfer processes.

4.4. Review on the fabricated OLED devices

Research on device fabrication started as OLED technology is the bright light of the flat panel displays industry. Introduction of rare earths results in a drastic improvement on the performance of luminescent devices. Kido and Nagai [132] fabricated red light emitting devices using tris(thenoyl trifluoro acetones)Eu^{3+} complex as the emitter. As this complex is not volatile the luminescent layer was fabricated by spin coating poly(methyl phenyl silane) film, which was molecularly doped with Eu^{3+} complexes. The cell structure was glass substrate/ITO/polysilane/electron transport layer/Mg/Ag. A sharp red electroluminescence was obtained at dc bias voltages of over 12 V.

In 1995, Sano et al. fabricated of multi-layer EL cell with the emission of a Eu-complex formed by vacuum-vapor deposition technique. They used 1AZM-HEX (host material) as a emitting layer and $Eu(TTA)_3Phen$ as a dopant. A red emission at 614 nm with very sharp spectral band was observed from the EL cell with 5 wt% of $Eu(TTA)_3Phen$ and maximum luminance of 137 cd/m^2 was achieved. Adachi et al. [133] investigated the energy mechanism for energy transfer leading to electroluminescence of lanthanide complex $Eu(TTA)_3Phen$ doped into 4-4′-N,N′-dicarbozole-biphenyl (CPB) host. They achieved maximum external quantum efficiency of 1.4% at a current density of 0.4 mA/cm^2 with the device structure of anode/HTL/$Eu(TTA)_3$ Phen (1%):CPB/ETL/cathode.

In 2001 Chen et al. [134] used series of tris-(8-hydroxyquinoline) metal chelates with central metal ions of Al^{3+}, Ga^{3+}, In^{3+} as the host materials. A red fluorescent dye, 4-(dicyanomethylene)-2-*t*-butyl-6-(8-methoxy-1,1,7,7-tetramethyl julolidyl-9-enyl)4H-pyran (DCJMTB) was used as the emitter or guest dopant material. The doped devices with Gaq_3 as the host materials produce high efficiencies and saturated red color chromaticity. The device with 1% DCJMTB doped in Gaq_3 showed a current efficiency of 2.64 cd/A. The color coordinates of the Gaq_3:1% DCJMTB device in the Commission international del'Eclairage chromaticity chart are $x = 0.63$ and $y = 0.36$.In 2002 Ma et al. [135] synthesized a novel red luminescent material BDCM (N,N-bis{4-[2-(4-dicyanomethylene-6-methyl-4H-pyran-2-yl) ethylene]phenyl}aniline) with two (4-dicyanomethylene)-4H-pyran electron-acceptor moieties and a triphenylamine electron-donor moiety for application in organic light-emitting diodes (OLEDs). The three-layered EL device with the structure ITO/CuPc/DPPhP/BDCM/Mg:Ag has a turn-on voltage of less than 4 V, which suggests that BDCM has an excellent electron injection property. A bright luminance of 582 cd/m^2 is obtained for the device at 19 V. Ohmori et al. [136] employed two kinds of

Table 4
Abbreviation, name and synonym of β-diketonates.

Abbreviation	Name	Synonym
4-picO	4-Picoline *N*-oxide	
bath	4,7-Diphenyl-1,10-phenanthroline	Bathophenanthro-line
bipy	2,2′-Bipyridine	
btfac	Benzoyl trifluoroacetone	
bzac	Benzoylacetone	1-Phenyl-1,3-butanedione
dbm	Dibenzoyl methane	
dbzso	Dibenzylsulfoxide	
diglyme	Diethyleneglycol Dimethyl ether	
dipydike	1,3-(2-Pyridyl)-propane-1,3-dione	
dipydike	1,3-(2-Pyridyl)-propane-1,3-dione	
distyphen	4,7-Distyryl-1,10-phenanthroline	
distyphen	4,7-Distyryl-1,10-phenanthroline	
dmbm	4-Methoxy dibenzoylmethane	4,4′-Dimethoxy-dibenzoylmethane
dme	Dimethoxyethane	
dmh	2,6-Dimethyl-3,5-heptanedione	
dmso	Dimethylsulfoxide	
dnm	Di(2-napthoyl)methane	1,3-Diphenyl-1,3-propanedione
dpphen	4,7-Diphenyl-1,10-phenanthroline	
fod	6,6,7,7,8,8,8-heptafluoro-2	2-Dimethyl-3,5-octanedione
Hacac	Acetylacetone	2,4-Pentanedione
Hbfa	Benzoyl-2-furanoylmethane	
Hbpp	1,3-Bis(3-pyridyl)-1,3-propanedione	
Hbtfac	Benzoyltrifluoroacetone	
Hbzac	Benzoylacetone	1-Phenyl-1,3-butanedione
Hdbbm	Di(4-bromo)benzoylmethane	
Hdbm	Dibenzoylmethane	
Hdbm	Dibenzoylmethane	1,3-Diphenyl-1,3-propanedione
Hdmbm	4,4′-Dimethoxydibenzoylmethane	
Hdmh	2,6-Dimethyl-3,5-heptanedione	
Hdnm	Dinaphthoylmethane	
hfac	Hexafluoroacetylacetone,	1,1,1,5,5,5-Hexafluoro-2,4-pentanedione
hfac	Hexafluoroacetylacetone,	1,1,1,5,5,5-Hexafluoro-2,4-pentanedione
Hfdh	6,6,6-Trifluoro-2,2-Dimethyl-3,5-hexanedione	
Hfhd	1,1,1,2,2,6,6,7,7,7-Decafluoro-3,5-heptanedione	
Hfod	6,6,7,7,8,8,8-Heptafluoro-2,2-dimethyl-3,5-octanedione	
Hftac	2-Furyltrifluoroacetone	4,4,4,-Trifluoro-1-(2-furyl)-1,3-butanedione
Hhfbc	3-(Heptafluorobutyryl)-*d*-camphor	
Hhfth	4,4,5,5,6,6,6-heptafluoro-1-(2-thienyl)-1,3-hexanedione	
Hmhd	6-Methyl-2,4-heptanedione	
Hntac	2-Naphthoyltrifluoroacetone	4,4,4-Trifluoro-1-(2-naphthyl)-1,3-butanedione
Hpbm	2-(2Pyridyl)benzimidazole	
Htfac	1,1,1-Trifluoro-2,4-pentanedione	Trifluoroacetyl-acetone
Hthd	2,2,6,6-Tetramethyl-3,5-heptanedione	
Htmod	2,2,6,6-Tetramethyl-3,5-octanedione	
Htod	2,2,7-Trimethyl-3,5-octanedione	3-Butanedione
mfa	4-Methoxybenzoyl-2-furanoylmethane	
mhd	6-Methyl-2,4-heptanedione	
monoglyme	Monoethyleneglycol dimethyl ether	
opb	1-Octadecyl2(2pyridyl) benzimidazole	
phen	1,10-Phenanthroline	
phenNO	1,10-Phenanthroline-*N*-oxide	
pip	Piperidine	
pta	Pivaloyltrifluoroacetone	5,5-Dimethyl-1,1,1-trifluoro-2,4-hexanedione
py	Pyridine	
pyO	Pyridine-*N*-oxide	
pyr	Pyrazine	
tbp	Tri-*n*-butylphosphate	
tbpo	Tri-*n*-butylphosphine oxide	
terpy	2,2′,6′,2′-Terpyridyl	
tetraglyme	tetraethyleneglycol dimethyl ether	
thd	2,2,6,6-Tetramethyl-3,5-heptanedione dipivaloylmethane	
topo	Tri-*n*-octylphosphine oxide	
tppo	Triphenylphosphine oxide	
triglyme	Triethyleneglycol dimethyl ether	
trimh	2,2,6-Trimethyl-3,5-heptanedione	
trimh	2,2,6-Trimethyl-3,5-heptanedione	
tta	2-Thenoyl trifluoro acetone	4,4,4-Trifluoro-1-(2-thienyl)-1,3-butanedione

material systems utilizing energy transfer and energy confinement: one, a co-doped OLED, which consists of two different kinds of materials doped in the emissive layer, and the other type a europium (Eu) complex (1,10-phenanthroline)-tris (4,4,4-trifluoro-1-(2-thienyl)-butane-1,3-dionate) europium(III), [Eu(TTA)$_3$phen] is doped in poly(N-vinylcarbazole) (PVK). Red light emission at 614 nm was obtained with efficient emission relaxation in Eu^{3+} sites.

Table 5
Melting and decomposition temperature of organic red emitting materials.

Organic materials	Melting and decomposition temperature (°C)	Ref.
[Eu(acac)$_3$](amorphous)	160–170	[93]
[Eu(acac)$_3$](crystalline)	94	[93]
[Eu(acac)$_3$(bipy)]	200–202	[94]
[Eu(acac)$_3$(H$_2$O)]	147–148	[95]
[Eu(acac)$_3$(distyphen)]	255–260	[96]
[Eu(acac)$_3$Phen]	250–255	[96]
[Eu(dbm)$_3$(bipy)]	210–213	[96]
[Eu(tta)$_3$(4-picO)$_2$]	234–236	[96]
[Eu(tta)$_3$(terpy)]	247–251	[96]
[Eu(tta)$_3$(tppo)$_2$]	251–253	[96]
[Eu(tpb)$_3$Phen]	197–199	[97]
[Eu(bzac)$_3$Phen]	192–194	[97]
[Eu(dbm)$_3$Phen]	184–187	[97]
[Eu(tta)$_3$Phen]	242–244	[97]
[Eu(tta)$_3$(bipy)]	221–223	[97]
[Eu(btfac)$_3$(H$_2$O)$_2$]	107–110	[98]
[Eu(btfac)$_3$(bipy)]	193–194	[99]
[Eu(bzac)$_3$(bipy)]	173–174	[99]
[Eu(btfac)$_3$Phen]	186–188	[99]
[Eu(dbm)$_3$(bath)]	191–192	[99]
[Eu(dnm)$_3$Phen]	215–216	[100]
[Eu(hfac)$_3$Phen]	257	[100]
[Eu(dbm)$_3$(dpphen)]	239–241	[100]
[Eu(dbm)$_3$Phen]	272–274	[100]
[Eu(btfac)$_3$(tppo)$_2$]	136	[101]
[Eu(bzac)$_3$(H$_2$O)$_2$]	100–104	[102]
[Eu(bzac)$_3$Phen]	186–188	[103]
[Eu(dbm)$_3$(aniline)]	206–209	[104]
[Eu(dbm)$_3$(n-butylamine)$_2$]	145–147	[104]
[Eu(dbm)$_3$(1,4-dioxane) $_2$]	170–175	[104]
[Eu(dbm)$_3$(dmf)]	133–138	[104]
[Eu(dbm)$_3$(dmso)$_3$]	112–115	[104]
[Eu(dbm)$_3$(piperidine)$_2$]	183–185	[104]
[Eu(dbm)$_3$(py)$_2$]	103–106	[104]
[Eu(dbm)$_3$(pyO)]	189–190	[104]
[Eu(dbm)$_3$(quinoline)$_2$]	109–111	[104]
[Eu(dbm)$_3$(opb)]	119	[105]
[Eu(dmh)$_3$(bipy)]	147–149	[106]
[Eu(dbm)$_3$Phen]	181–183	[106]
[Eu(fod)$_3$]	205–212	[107]
[Eu(fod)$_3$(H$_2$O)]	59–67	[107]
[Eu(fod)$_3$(bipy)]	68–73	[108]
[Eu(fod)$_3$Phen]	97–99.5	[108]
[Eu(fod)$_3$(py)$_2$]	70.5–72	[108]
[Eu(fod)$_3$(4-picO)]	193.5–194.5	[108]
[Eu(fod)$_3$(tppo)$_2$]	220.5–223	[108]
[Eu(fod)$_3$(bipy)]·2H$_2$O	78	[109]
[Eu(hfac)$_3$]	176–177	[110]
[Eu(thd)$_3$]	190–191	[110]
	157	[111]
[Eu(hfac)$_3$]2H$_2$O	181–182	[112]
	110	[113]
[Eu(mhd)$_3$Phen]	186–189	[114]
[Eu(pta)$_3$]	113.8–114	[115]
[Eu(thd)$_3$(dme)]	176–178	[116]
[{Eu(thd)$_3$}2(tetraglyme)]	98–100	[116]
[{Eu(thd)$_3$}2(triglyme)]	111–114	[116]
[Eu(thd)$_3$Phen]	230–231	[117]
[Eu(thd)$_3$(py)]	135–138	[118]
[Eu(thd)$_3$(pyr)]	211–214	[119]
[Eu(trimh)$_3$]	182–183	[120]
[Eu(tta)$_3$]	180	[121]
[Eu(tta)$_3$(opb)]	95–98	[122]

Qu et al. [137] synthesized two novel polymers PQP (poly(3,7-N-octyl phenothiozinyl cyanoterephthalylidene)) and PQM (poly(3,7-N-octyl phenothiozinyl cyanoisophthalylidene)) containing phenothiazine for application in red and orange light-emitting diodes. The single-layer EL devices of indium tin oxide (ITO)/PQP (or PQM)/Mg:Ag and multi-layer devices of ITO/PQP (or PQM): N,N′-diphenyl-N,N′-bis(3-methylphenyl)-[1,1′-biphenyl]-4,4′-diamine(TPD) (44 nm)/2, 9-dimethyl-4,7-diphenyl-1,10-phenanthroline (BCP, 5 nm)/tris(8-hydroxyquinolinato) aluminium (AlQ_3, 20 nm)/Mg:Ag were fabricated. The EL spectra from the devices based on PQP, PQM peaked at the wavelength of 664 nm, 608 nm with maximum brightness of 60 cd/m^2, 150 cd/m^2 for applied voltage of 17 V and 14 V, respectively.

A blue organic light-emitting diode employing perylene as light emitting dopant and 9,10-bis(3′5′-diaryl)phenyl anthracene (DPA) as host has been studied for its decay mechanisms. The device structure is ITO indium tin oxide/CuPcs copper phthalocyanined/NPDsa-naphthylphenylbiphenyl diamined/DPA:perylene/Alq_3 (8-hydroxy-quinoline aluminum)/MgAg. A luminance of 4359 cd/m^2 at 15 V and a current efficiency of 3 cd/A at 5 V have been achieved [138].

A new series of pyrazoloquinoline copolymers with N-vinylcarbazole were synthesized [139], these materials possess high quantum efficiency (up to 1.16%) in blue spectral range (440–480 nm). The copolymers possess principal advantageous compared to the traditional polymers mixtures due to substantially higher stability and larger quantum efficiency. It is crucial that appropriately varying the pyrazoloquinoline derivative substitution they observed a red spectral shift of the electroluminescent maxima possessing the enhanced quantum efficiency.

For the application in OLEDs, efficient new red phosphorescent iridium(III) complexes, bis[2,3-diphenyl-4-methyl-quinolinato-C2,N] iridium(III) acetylacetonate [Ir(4-Me-2,3-dpq)$_2$(acac)] and bis[2,3-di(4-methoxy-phenyl)-4-methyl-quinolinato-C2,N] iridium(III) acetyl acetonate [Ir(4-Me-2,3-dpq(OMe)$_2$)$_2$(acac)] were synthesized[] from the two-step reactions of $IrCl_3{\cdot}xH_2O$ with the corresponding ligand by Park and Ha [72]. The complexes exhibited the luminescence peak at 604 and 592 nm, respectively. Electroluminescent (EL) devices with a configuration of ITO/2-TNATA/NPB/CBP:dopant/BCP/AlQ_3/Liq/Al were also fabricated. The Commission Internationale de L'Eclairage (CIE) coordinates of Ir(4-Me-2,3-dpq)$_2$(acac) and Ir(4-Me-2,3-dpq(OMe)$_2$)$_2$ (acac) were (0.644, 0.352) and (0.615, 0.375), respectively.

In 2009 Seo et al. [74] fabricated OLEDs using red novel phosphorescent hetero leptic tris cyclometalated iridium complex, bis(2-phenylpyridine)iridium(III)[2(5-methylphenyl)-4-diphenylquinoline] [Ir(ppy)$_2$ (dpq-5CH$_3$)], based on 2-phenylpyridine (ppy) and 2(5-methylphenyl) 4-diphenyl quinoline (dpq-5CH$_3$) ligand. They demonstrated that high efficiency through the sensitizer can be obtained, when T_1 of the emitting ligand is close to T_1 of the sensitizing ligand. The device containing Ir(ppy)$_2$(dpq–5CH$_3$) produced red light emission of 614 nm with maximum luminescence efficiency and power efficiency of 8.29 cd/A (at 0.09 mA/cm^2) and 5.79 lm/W (at 0.09 mA/cm^2), respectively.

Blue phosphorescent iridium complexes based on 2-(fluoro substituted phenyl)-4-methylpyridines were synthesized by Xu et al. [140]. They proved that the introduction of fluorine atoms and methyl group into ppy ligand and changing in position of F substituent's in phenyl ring can finely tune emission of the complexes, showing bright blue-to-green luminescence at a wavelength of 463–501 nm at room temperature in CH_2Cl_2.

Blue organic light-emitting diodes with low driving voltage and maximum enhanced power efficiency based on wide band gap host material, 2-(t-butyl)-9,10-di-(2-naphthyl) anthracene (TBADN), blue fluorescent styrylamine dopant, p-bis(p-N,N-diphenyl-amino-styryl)benzene (DSA-Ph) have been realized by using molybdenumoxide(MoO_3) as a buffer layer and 4,7-diphenyl-1,10 phenanthroline (BPhen) as the ETL. The typical device structure used by Haq et al. [141] was glass substrate/ITO/MoO_3(5 nm)/NPB (30 nm)/[TBADN:DSA-Ph (3 wt%)](35 nm)/BPhen (12 nm)/LiF(0.8 nm)/(100 nm). It was found that the MoO_3 JBPhen based device shows the lowest driving voltage and highest power efficiency among the referenced

devices. At the current density of 20 mA/cm^2, its driving voltage and power efficiency are 5.4 V and 4.7 Lm/W, respectively.

OLEDs with high efficiency, low driving voltage and saturated red color realized via two step energy transfer based on ADN and Alq_3 co-host system with the typical device structure was glass substrate/ITO/4,40,400-tris(N-3-methylphenyl-N-phenyl amino) triphenylamine (m-MTDATA)/N,N0-bis (naphthalene-1-yl)-N, N0-diphenyl-benzidine (NPB)/[ADN:Alq_3]: DCJTB:C545T/Alq_3/LiF/Al. Current efficiency of 3.6 cd/A, Commission International d'Eclairage coordinates of [0.618, 0.373] and peak λ_{max} = 620 nm at a current density of 20 mA/cm^2 was achieved [142].

In 2009 Wu et al. [143] synthesized and characterized a novel blue-emitting material, 2-tert-butyl-9,10-bis[40-(9-ptolyl-fluoren-9-yl)biphenyl-4-yl]anthracene (BFAn), containing an anthracene core end-capped with 9-phenyl-9-fluorenyl groups. OLEDs featuring BFAn as the emitter exhibited an excellent external quantum efficiency of 5.1% (5.6 cd/A) with CIE coordinates of (0.15, 0.12) that are very close to the National Television Standards Committee's blue standard. The power efficiency of our BFAn-based devices reached as high as 5.7 lmW_1, making them superior to other reported non-doped deep-blue OLEDs. Two new blue emitting materials of o,p-TP-EPY (6,6,12,12-tetraethyl-2,8-bis-[1,1;3,1]terphenyl-4-yl-6,12-dihydro-diindeno[1,2-b;1,2-e]pyrazine) and m,m-TP-EPY (6,6,12,12-tetraethyl-2,8-bis-[1,1;3,1]terphenyl-5-yl-6,12-dihydro-diindeno[1,2-b;1,2-e]pyrazine) were synthesized using two bulky mterphenyl side groups with different substitution positions in the new core system of indenopyrazine (IPY). The o,p-TP-EPY more effectively prevented intermolecular interactions compared to m,m-TP-EPY, resulting in more blue-shifted emission in the thin film state. When the synthesized compounds were used as emitting layers in non-doped OLED devices [144], an identical trend in electroluminescent spectra was observed. EL spectrum of o,p-TP-EPY (max, EL = 440 nm) was more blue shifted than that of m,m-TP-EPY (max, EL = 452 nm), and external quantum efficiency (E.Q.E.) of o,p-TP-EPY (2.68%) was also showed large improvement of about 60% compared to efficiency of m,m-TP-EPY (1.61%). Deep blue organic light-emitting diodes based on triphenylenes were fabricated by Wettach et al. [145] with photoluminescence emission spectra at around 400 nm. Cho et al. [146] fabricated OLED devices in 2010, with 10% of Ir(Cz-ppy)$_1$(Cz-Fppy)$_2$ in PVK/PBD (70:30 wt%), exhibited an external quantum efficiency of 6.80%, luminous efficiency of 20.23 cd/A, and maximum brightness of 17520 cd/m^2.

A novel deep-red-emitting iridium complex Ir(ppy)$_2$(BYNO)[80] (ppy: 2-phenylpyridine) with single-peaked narrow emission band was fabricated by Guang et al. with efficient deep red emission peaking at 620 nm and narrow emission band (full-width-at-half-maximum 65 nm) from Ir(ppy)$_2$(BYNO). Maximum luminance of 3840 cd/m^2 peaking at 618 nm is achieved. In 2011 Zhang et al. [147] demonstrated the design and fabrication of solution processed white light-emitting diodes (LEDs) containing a bilayer of heavy metal-free colloidal quantum dots (QDs) and polymer in the device active region. White electroluminescence was obtained in the LEDs by mixing the red emission of ZnCuInS/ZnS core/shell QDs and the blue-green emission of poly(N,N0-bis(4-butylphenyl)-N,N0-bis(phenyl)benzidine).Blue top-emitting organic light-emitting devices (TEOLEDs) based on blue phosphor iridium(III) bis[(4,6-difluorophenyl)-pyridinato-N,C20] picolinate (FIrpic) are demonstrated by Xie et al. [148]. Blue emission with a good chromaticity is achieved through the suppression of the multiple-beam interference by introducing a 2,9-dimethyl-4,7-diphenyl-1,10-phenanthroline light out coupling layer onto the semitransparent Sm/Ag cathode. Maximum luminance of 8029 cd/m^2 and a luminous efficiency of 4.02 cd/A was achieved at 14 V and 10 V, respectively.

High-efficiency OLEDs were fabricated by Kim et al. [149] in which solution processed ambipolar blends of hole- and electron-transport polymer hosts doped with a green-emitting iridium complex are sandwiched between a photocrosslinked hole-transporting layer and a vacuum-deposited electron-transporting layer. The ambipolar host blends consist of blends of bis-oxadiazole-functionalized poly(norbornene) electron-transport materials and poly(N-vinylcarbazole). External quantum efficiency of 13.6% and a maximum luminous efficiency of 44.6 cd/A at 1000 cd/m^2 with a turn-on voltage of 5.9 V were obtained.

Thejo Kalyani et al. [150] fabricated red OLED devices with the device structure of anode/hole transport layer/$Eu_xY_{(1-x)}$(TTA)$_3$Phen (15%): TPBi/electron transport layer/cathode, maximum luminescence of 185.6 cd/m^2 and 44.72 cd/m^2 was obtained from device I made of $Eu_{0.4}Y_{0.6}$(TTA)$_3$Phen and device II made of $Eu_{0.5}Y_{0.5}$(TTA)$_3$Phen, respectively at 18 V. Saturated red Eu^{3+}emission based on $^5D_0 \rightarrow {}^7F_2$ transition is centered at a wavelength of 612 nm with a full width at half maximum of 5 nm.

5. White OLEDs

White organic light-emitting diodes (WOLEDs) are of growing interest for the next generation of displays and solid-state lighting technologies owing to their low-cost, high-efficiency and flexible properties [151–157]. Single-layer white polymer light-emitting diodes based on an iridium(III) complex containing alkyl trifluorene picolinic acid was fabricated by Yafei Wang [158]. White light-emitting diodes (WLEDs) are considered as the third generation (3G) lighting sources because of their excellent properties such as low energy consumption, extremely long life, high durability and mercury free [159–163]. To obtain high brightness WLED, mainly blue emitting LED is used in combination with yellow phosphor to partially down convert the blue emission into light with longer wavelengths.

As a promising candidate for lighting source, white OLEDs should generate light with spectral distribution similar to that of natural sunlight covering the full visible range as much as possible. For lighting purpose, the light sources should give CIE coordinates closer to the ideal white point at (0.33, 0.33) for better color purity. White-light emission is usually observed by a set of different luminophores with distinct emission colors, typically two (blue and orange/yellow) or three (blue, green and red). Fig. 9 represents the general strategies so far developed for the devices to combine multiple emitters in the EML to produce white light. They include.

5.1. WOLEDs from R-G-B primary colors

The three primary color (red, blue, green) phosphors can be doped into either one or several layers to form WOLEDs with single and multi-EMLs, respectively. So, all-phosphorescent WOLEDs with R-G-B emitters can fall into two main categories.

5.2. Single-EML WOLEDs with R-G-B primary colors

It is simple to make WOLEDs by doping R-G-B phosphors into a single-EML, which can be obtained by either vacuum deposition or low-cost solution-process strategy. In both cases, special attention should be paid to prevent phase separation so that a homogeneous EML can be formed which would help to extend the lifetime of the devices. Doping three emitters into a single layer would probably induce energy transfer processes from the short-wavelength emitters to the longer-wavelength ones, which would result in a color shift with respect to driving voltage or brightness and thus impair the quality of the white light. Generally, the doping level for blue

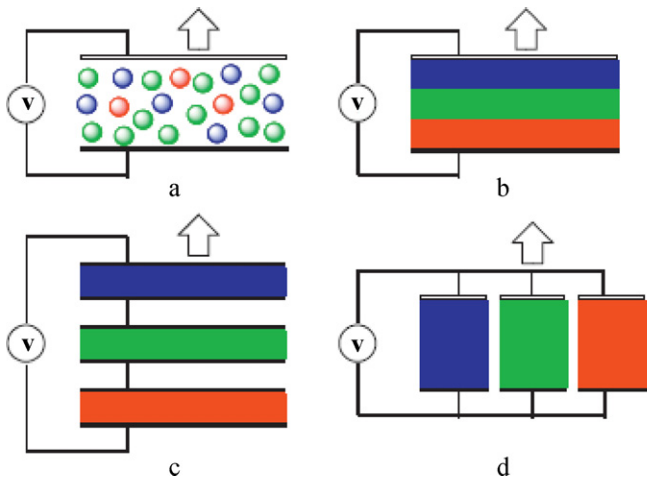


Fig. 9. General approaches to generate white light from OLEDs using multiple emitters. (a) Single-EML structure, (b) multilayer EML structure, (c) stacking and tandem structure and (d) striped structure.

Reproduced from Zhou et al., Recent progress and current challenges in phosphorescent white organic light-emitting diodes (WOLEDs), J. Photochem. Photobiol. C: Photochem. Rev. (2011), doi:10.1016/j.jphotochemrev.2011.01.001.

phosphor is much higher than that of the green and red counterparts in order to maintain a more balanced R-G-B light component in the white EL spectrum.

5.3. Multi-EML WOLEDs with R-G-B primary colors

In this, the three primary color (red, blue, green) phosphors are doped as separate layers to form WOLEDs.

5.4. WOLEDs from B–O complementary colors

Besides R-G-B phosphorescent emitters, phosphors showing complementary colors, such as blue (B) and orange (O), can also be utilized to produce white-light emission in the devices. By reducing the number of phosphors used, the device fabrication process can be generally simplified. Owing to the absence of green-emitting phosphor, the CRI is usually moderate for the white light emitted from the WOLEDs with B–O complementary-colors. WOLEDs attract much research attention for their relatively simple device configuration, making the device fabrication simple as the process reduces the number of phosphors used.

5.5. Single-EML WOLEDs with B–O complementary colors

Like R-G-B single-EML WOLEDs, the phosphors in a B–O complementary-color configuration can be doped in either polymeric or small molecular host to form EML by solution process or vacuum deposition process. Similarly, the doping level for the phosphors also needs to be carefully controlled to achieve a desirable white EL spectrum. Recently, Wu et al. prepared a series of simple solution-processed WOLEDs by doping two phosphors of complementary colors into a host of PVK doped with OXD-7 to afford very high EL efficiencies [164]. By combining blue emitter FIrpic and orange one$(fbi)_2Ir(acac)$, Wang et al. have prepared high performance WOLEDs with single-EML by vacuum deposition [165]. By doping each of the two phosphors exhibiting B–O complementary colors into different EMLs, WOLEDs with multi-EMLs can be fabricated. General approaches to generate white light from OLEDs using multiple emitters. (a) Single-EML structure, (b) multilayer EML structure, (c) stacking and tandem structure and (d) striped structure are illustrated in Fig. 9.

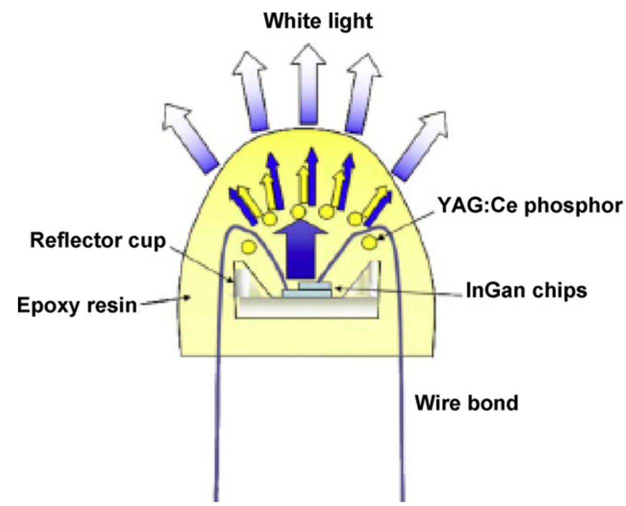


Fig. 10. Schematic of phosphor converted white light emitting diodes (pc-WLEDs).

5.6. Multi-EMLWOLEDs with B–O complementary colors

By doping each of the two phosphors exhibiting B–O complementary colors into different EMLs, WOLEDs with multi-EMLs can be fabricated. This may be relatively complicated device manufacturing compared to that of the single-EML WOLEDs, but double-EML devices can offer more flexibility to improve EL performance through fine optimization of every single-EML .Yu et al. developed double-EML WOLEDs consisting of blue Fir-pic phosphor and a functionalized orange emitter $Ir(DPA\text{-}Flpy)_3$ showing good HI/HT features [166]. The threshold voltage of the device is 4.2 V, and the brightness can reach 3200 cd/m^2 at 10 V. A schematic of phosphor-converted white light-emitting diodes (pc-WLEDs) is shown in Fig. 10 [160]. Fig. 11 shows three different methods of generating white light from LEDs.

6. Key challenges in OLEDs

Despite the progress made in the past decade and the first displays appearing in the market, major hurdles still exist which have to be overcome to make organic EL displays unique in comparison to the other FPD technologies. These challenges can be divided into four categories

6.1. Material issues

This includes the availability of higher purity materials (for both small molecule and polymer emitters), the necessity of higher efficiency and longer operating lifetimes for red and blue emitting materials, an ongoing improvement of the materials thermal stability and the requirement of more saturated colors to reach the NTSC (National Television standards Committee) norms. Improved large area shadow mask pattering techniques for small molecules.

6.2. Patterning techniques

Patterning techniques are required with a resolution down to ~50 μm. Simultaneously the masks should not damage any of the underlying layers and must be easily maintained and cleaned. Alternatively, the ink jet printing method needs further improvements in order to achieve a higher pixel fill factor.

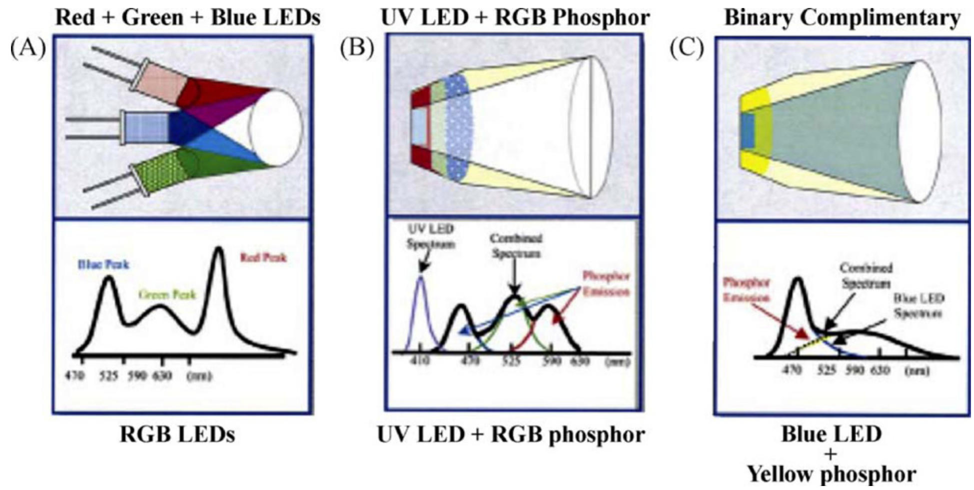


Fig. 11. Three methods of generating white light from LEDs: (a) red + green + blue-LEDs, (b) UV-LED + RGB phosphors, and (c) blue-LED + yellow phosphor. (For interpretation of the references to color in this figure legend, the reader is referred to the web version of the article.)

6.3. Driving circuits

For passive matrix driven OLED displays power losses in the driver circuits must be reduced. For higher information content displays, active matrix driving circuits with separate thin film transistors (TFTs) for switching and current control (i.e., at least two TFTs for each OLED pixel) are needed. The higher current requirements, however, necessitate the use of poly-Si TFTs.

6.4. Processing and manufacturing issues

From the manufacturing point of view, processing procedures that have a high through output and use low cost equipment are a prerequisite. During device fabrication a stringent contamination control is indispensable, particularly for conducting particles, which cause shorts as well as for oxygen and moisture.

The attributes such as high pixel to pixel contrast, high achievable brightness at low voltages, low power consumption, wide viewing angle, together with ultra high resolution capabilities make them ideal candidates to replace current established FPD technologies such as VFDs and LCDs. In comparison to early stages of the current LCD technology, OLEDs have the great advantage that they can make full use of the existing LCD process technology experiences. In addition, the ability to fabricate OLEDs on flexible and bendable substrates of arbitrary shapes makes them unique in comparison to the other FPD technologies.

7. Research work undertaken

After deep review of literature we have synthesized, characterized rare earth based europium organic complexes and also fabricated OLED devices. In the present work, TTA(2-Thenoyltrifluoroacetone) has been selected as a ligand; a β-diketonates with aromatic and hetero cyclic substituent. Though the synthesized $Eu(TTA)_3$ complex is excellent red phosphors, it cannot be deposited by vacuum deposition technique, which is a popular and conventional method for fabricating an organic cell, as this is not volatile. Hence, another ligand has been selected namely Phen (1,10 phenanthroline), a Lewis base that can form adducts with rare earth tris β-diketonates. The so formed new volatile $Eu(TTA)_3Phen$ complex is based on synergistic effect and can be used for device fabrication by vacuum evaporation technique. Volatile pure europium complex $Eu(TTA)_3Phen$, yttrium and terbium doped europium binuclear complexes, namely $Eu_{(x)}Y_{(1-x)}(TTA)_3Phen$ and $Eu_{(x)}Tb_{(1-x)}(TTA)_3Phen$ have been synthesized by solution technique, maintaining stoichiometric ratio. Various characteristics such as structural confirmation, thermal stability and optical UV–vis absorption, photoluminescence (PL) for the synthesized rare earth complexes were carried out. Structural properties of the synthesized $Eu(TTA)_3Phen$, $Eu_{(x)}Tb_{(1-x)}(TTA)_3Phen$ and $Eu_{(x)}Y_{(1-x)}(TTA)_3Phen$ complexes were studied by XRD measurements, which reveal the crystalline or amorphous nature of the complex. Thermal stability, chemical reactivity and phase transition measurements were investigated by TGA/DTA measurements. TGA measurements reveal the specimen weight changes as a function of time and temperature in various gaseous environments while DTA is used for measuring in specimen heat content during heating and cooling cycles.

7.1. Reagents and solvents

All reagents and solvents used are of analytical reagents (AR) grade. Starting materials used for the synthesis of $Eu(TTA)_3Phen$, $Eu_{(x)}Y_{(1-x)}(TTA)_3Phen$ and $Eu_{(x)}Tb_{(1-x)}(TTA)_3Phen$ complex are europium chloride ($EuCl_3$), [rare earth chemicals] Purity – 99.5%, M.Wt = 258.32 g/mol. Yttrium chloride (YCl_3), [rare earth chemicals] purity – 99.5%, M.Wt = 195.26 g/mol. Terbium chloride ($TbCl_3$), [rare earth chemicals] Purity – 99.5%, M.Wt = 265.28 g/mol. 2-thenoyl trifluoroacetone ($C_8H_5F_3O_2S$), [national chemical], purity – 99.5%, M.Wt = 222.19 g/mol, b.p. (8 mmHg) = 96–98 °C, m.p. = 40–44 °C. 1–10 phenanthroline ($C_{12}H_8N_2H_2O$), [Merck company] purity – 99.5%, M.Wt = 198.22 g/mol, m.p. = 1000–1040 °C. Ethanol absolute (C_2H_5OH), purity – 99.98%, M.Wt = 46.07 g/mol. Potassium hydroxide (KOH), purity – 99.98%. 1 N of KOH = 5.611 g in 100 ml distilled water. Double distilled water. PMMA $[-CH_2C(CH_3)CO_2CH_3-]_n$, polystyrene $[-CH_2CH(C_6H_5)-]_n$ and chloroform ($CHCl_3$, 99.5%). Structure of 2-thenoyl trifluoro acetone and 1–10 phenanthroline is as shown in Fig. 12(a) and (b), respectively.

7.2. Structure and synthesis of organic complexes

Fig. 13 shows the chemical structure of $Eu(TTA)_3Phen$, it is clear that 1:10 phenanthroline and TTA are bidendate. Eu^{3+} is associated with three molecules of TTA and one molecule of Phen. Eu^{3+} has 8 co-ordinates (6 with TTA, which are shown to the right of Eu^{3+} while

Table 6
The composition of the chemical constituent for the synthesis of $Eu_{(x)}Y_{(1-x)}(TTA)_3$Phen complexes.

Complexes $Eu_{(x)}Y_{(1-x)}(TTA)_3$Phen	TTA in (g)	Phen in (g)	$EuCl_3$ in (g)	YCl_3 in (g)
$x = 0.4$	1.4731	0.4381	0.2283	0.2589
$x = 0.5$	1.4731	0.4381	0.2854	0.2157

Table 7
The composition of the chemical constituent for the synthesis of $Eu_{(x)}Tb_{(1-x)}(TTA)_3$Phen complexes.

$Eu_{(x)}Tb_{(1-x)}(TTA)_3$Phen	TTA in (g)	Phen in (g)	$EuCl_3$ in (g)	$TbCl_3$ in (gm)
$x = 0.4$	1.4731	0.4381	0.22831	0.3517
$x = 0.5$	1.4731	0.4381	0.28544	0.2931

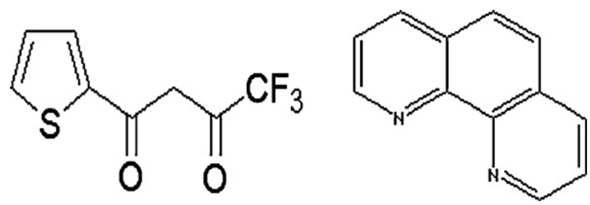


Fig. 12. Structure of (a) 2-thenoyl trifluoroacetone and (b) 1-10 phenanthroline.

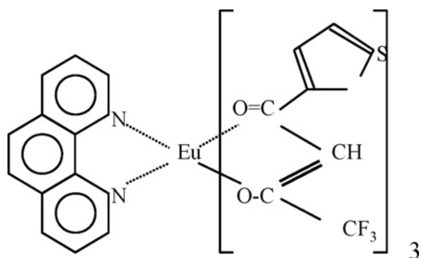


Fig. 13. Chemical structure of $Eu(TTA)_3$Phen.

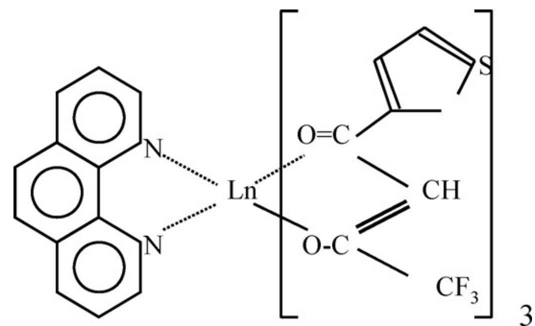


Fig. 14. Chemical structure of $Eu_{(x)}Ln_{(1-x)}(TTA)_3$Phen, where $x = 0.4$, 0.5, Ln = Y/Tb.

the other two with Phen, which are shown to the left of Eu^{3+}). The chemical structure of $Eu_{(x)}Ln_{(1-x)}(TTA)_3$Phen is shown in Fig. 14. $Eu_{(x)}Ln_{(1-x)}$ is associated with three molecules of TTA and one molecule of Phen. Hence, for the formation of $Eu(TTA)_3$Phen and $Eu_{(x)}Ln_{(1-x)}(TTA)_3$ complexes, the stichiometry of chemical compounds must be in 1:3:1 ratio. The outline of synthesis process of $Eu(TTA)_3$Phen is shown in Fig. 15. Similarly $Eu_{(x)}Ln_{(1-x)}(TTA)_3$Phen complexes (where $x = 0.4$, 0.5) were synthesized by taking total combination of $Eu_{(x)}Ln_{(1-x)}$ as 2.21 mol by dissolving in 10 ml of double distilled water in another flask. The composition of the chemical constituent for the synthesis of $Eu_{(x)}Y_{(1-x)}(TTA)_3$Phen and $Eu_{(x)}Tb_{(1-x)}(TTA)_3$ Phen complexes is shown in Tables 6 and 7, respectively.

The synthesized powder was purified by train sublimation method. In this method, the complexes were sublimed inside a quartz tube at 350 °C, under high vacuum (10^{-6} Torr) and the lighter impurities were diffused away by leaving the residues in the boat itself. The sublimed, highly purified complexes were then collected from the walls of the quartz boat.

Pure $Eu(TTA)_3$Phen complex and doped Eu binuclear complexes namely $Eu_{(x)}Y_{(1-x)}(TTA)_3$Phen, and $Eu_{(x)}Tb_{(1-x)}(TTA)_3$Phen, where $x = 0.4$ and 0.5 by solution technique according to stichiometric ratio. Various characterization techniques such as XRD, TGA/DTA, PL spectra, which reveal different parameters of the complexes were carried out. All the synthesized complexes display well resolved multiple peaks, revealing the crystalline nature of the complexes. For all the synthesized complexes maximum peak for 100% relative intensity was almost same with slightly different d-values. TGA and DTA measurements reveal that yttrium/terbium doped Eu complexes showed better stability and higher melting point than the pure Eu complex. Among all the synthesized complexes $Eu_{0.4}Tb_{0.6}(TTA)_3$Phen complex showed maximum stability while, $Eu_{0.5}Tb_{0.5}(TTA)_3$Phen shows melting point at higher temperature. PL emission spectra of all the synthesized complexes were carried out under an excitation wavelength of 370 nm. Emission spectra of the synthesized complexes show emission bands corresponding to ${}^5D_0 \rightarrow {}^7F_j$ transitions. The intensity of the electric dipole allowed ${}^5D_0 \rightarrow {}^7F_2$ transition is much stronger than the magnetic dipole allowed transition ${}^5D_0 \rightarrow {}^7F_1$ indicating that Eu^{3+}

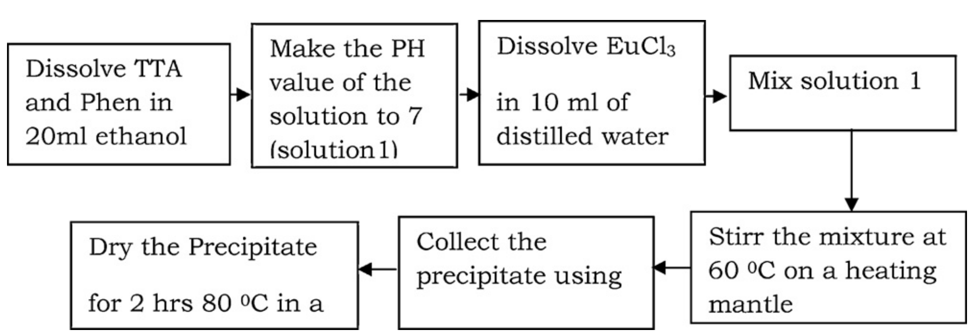


Fig. 15. Outline of the synthesis process of $Eu(TTA)_3$Phen.

Table 8
Structural, thermal and optical properties of $Eu(TTA)_3Phen$, $Eu_{(x)}Y_{(1-x)}(TTA)_3Phen$ and $Eu_{(x)}Tb_{(1-x)}(TTA)_3Phen$ complexes.

Parameter	$Eu(TTA)_3Phen$	$Eu_{0.5}Y_{0.5}(TTA)_3Phen$	$Eu_{0.4}Y_{0.6}(TTA)_3Phen$	$Eu_{0.5}Tb_{0.5}(TTA)_3Phen$	$Eu_{0.4}Tb_{0.6}(TTA)_3Phen$
Molecular formula	$EuC_{36}H_2O\ S_3F_9N_2O_6$	$Eu\text{-}YC_{36}H_2O\ S_3F_9N_2O_6$	$Eu\text{-}YC_{36}H_2O\ S_3F_9N_2O_6$	$EuTbC_{36}H_2O\ S_3F_9N_2O_6$	$EuTbC_{36}H_2O\ S_3F_9N_2O_6$
Appearance	Pale yellow	Pale yellow	Pale yellow	Pale yellow	Pale yellow
Molecular weight	1117.0521	1085.53	1079.22	1120.51	1121.20
Nature	Crystalline	Crystalline	Crystalline	Crystalline	Crystalline
d-Values[a] (Å)	9.99	9.67	9.74	9.7	9.96
Angle 2θ[a] (Å)	10.5	10.5	10.5	10.5	10.25
Peak intensity[a] (counts)	261	410	435	475	305
Stability of complex (°C)	333.63	335.54	340.09	333.87	336.28
Melting point (°C)	244.61	246.45	245.74	248.85	247.78
Excitation wavelength (nm)	370	370	370	370	370
Emission wavelength (nm)	611	611	611	611	611
Emission intensity (a.u.)	375	500	604	400	460

[a] 100% relative intensity.

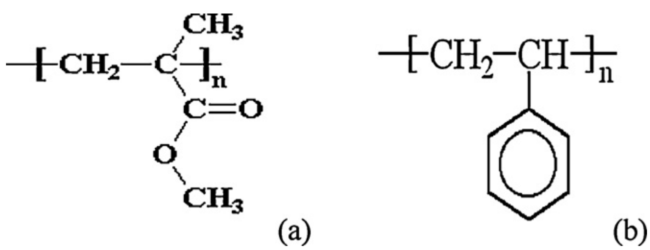


Fig. 16. Molecular structure of (a) PMMA and (b) polystyrene.

Table 9
Physical and chemical parameters of PMMA and PS.

Parameter	Polymethylmethacrylate	Polystyrene
Chemical formula	$(C_5O_2H_8)_n$	$(C_8H_8)_n$
Synonyms	PMMA poly(methyl methacrylate)	PS
Molecular mass	Varies	Varies
Density	$1.19\ g/cm^3$	$1.05\ g/cm^3$
Melting point	180 °C	237.5 °C
Boiling point	200.0 °C	–
Glass transition	114 °C	100 °C
Refractive index	1.492 (λ = 589.3 nm)	1.519 (λ = 589.3 nm)
Transmission	80–90%	–

ions occupy very low symmetric sites in these complexes. Among all the synthesized complexes, maximum PL emission intensity of 604 (a.u) counts was observed for $Eu_{0.4}Y_{0.6}(TTA)_3Phen$ at 611 nm. This enhancement in emission intensity may be attributed due to the introduction of Y^{3+} metal ion in $Eu(TTA)_3Phen$. As the synthesized complexes are crystalline, thermally stable and exhibit intense emission bands at 611 nm, these complexes can be used to fabricate red OLED devices, which can be employed in flat panel displays, optoelectronic devices where red Structural, thermal and optical properties of $Eu(TTA)_3Phen$, $Eu_{(x)}Y_{(1-x)}(TTA)_3Phen$ and $Eu_{(x)}Tb_{(1-x)}(TTA)_3Phen$ complexes are compared in Table 8.

In the present work, molecular doping method of organic complexes with a polymer has been considered. Polymethylmetacrylate (PMMA) and polystyrene (PS) were chosen as model polymers as they have a good film forming properties with a high glass transition temperature of 105 °C and 100 °C, respectively. PMMA is a common polymer, stable in air with a high formability, and have no absorption and fluorescence in the visible region. The molecular structure of PMMA is shown in Fig. 16(a). PMMA although being a linear polymer, it forms the quasi-cross-linked structure through strong dipole–dipole interactions, preventing it from crystallization [167,168]. Polystyrene is a lightweight cellular plastic foam material composed of carbon and hydrogen atoms. The molecular structure of PS is shown in Fig. 16(b). The polystyrene when undergoes glass transition, becomes flexible rather than rigid. As both polymers have good film forming properties with a high glass transition temperature, the synthesized Eu complexes are molecularly doped in PMMA and PS. The physical and chemical parameters of PMMA and PS were shown in Table 9.

7.3. Preparation and characterization of blended films

Commercially available polymers PMMA/PS were used for making blended films of the synthesized complexes. Polymer (PMMA/PS) matrix is prepared by dissolving 0.5 g of polymer (PMMA/PS) in 15 ml of chloroform with vigorous stirring for 15 min at room temperature. Later 0.05 g of the synthesized complex of pure $Eu(TTA)_3Phen$, $Eu_{0.5}Y_{0.5}(TTA)_3Phen$ and $Eu_{0.5}Tb_{0.5}(TTA)_3Phen$ was taken individually and dissolved in the same solvent in separate beakers. Later, the complex solution was mixed with PMMA/PS matrix at room temperature under vigorous stirring for 15 min to obtain the homogeneous mixture. The resulting homogeneous mixture is then poured on to a glass or good quality stainless steel substrate. The solvent is allowed to evaporate in air for 2–3 h at room temperature and then pilled up from the substrate. The obtained films are placed in vacuum dry oven at room temperature overnight to remove residual solvent left, if any. The obtained blended films are homogeneous and showed excellent optical transparency. No visible phase separation is detected. Absorption and photo luminescence measurements were recorded on SPECORD 50 spectrophotometer and Hamamatsu F-4500 spectrofluorometer, respectively.

7.4. Determination of energy gap

Blended films of pure and doped Eu complexes molecularly doped into polymer resins namely polymethylmetacrylate (PMMA) and polystyrene (PS) are prepared according to weight percentage. Absorption spectra of doped PMMA/PS systems were recorded on Analytic SPECORD 50 spectro photometer for 10 wt%. Absorbance spectra of blended films in PMMA are characterized by a two absorption peaks centered at 334 nm and 280 nm as shown in Fig. 17. The absorption peak at 334 nm is attributed to the π–π^* transition of β-diketonate ligand TTA, while the other peak at 280 nm is attributed to the π–π^* transition of Eu^{3+} β-diketonate (TTA) moieties, showing that all compounds have the same tris chelated core. As the absorption wavelength is the characteristic of aromatic group of β-diketonate (TTA), λ_{max} in all complexes appear at the same position with a change in the optical density.

Using the procedure described by Morita et al. [169], for energy gap determination, a plot between energy and $(energy \times absorbance)^2$ is plotted for the complexes in PMMA as shown in Fig. 18. The cutting edge of the plot on x-axis is

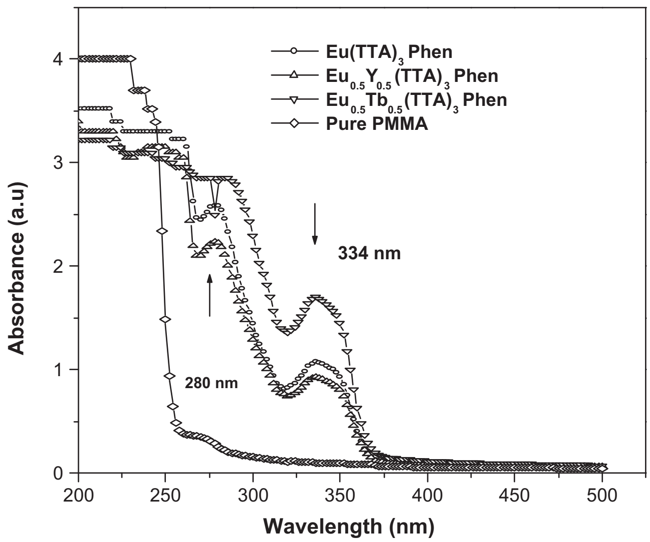


Fig. 17. Absorption spectra of $Eu(TTA)_3Phen$, $Eu_{0.5}Y_{0.5}(TTA)_3Phen$ and $Eu_{0.5}Tb_{0.5}(TTA)_3Phen$ blended films in PMMA.

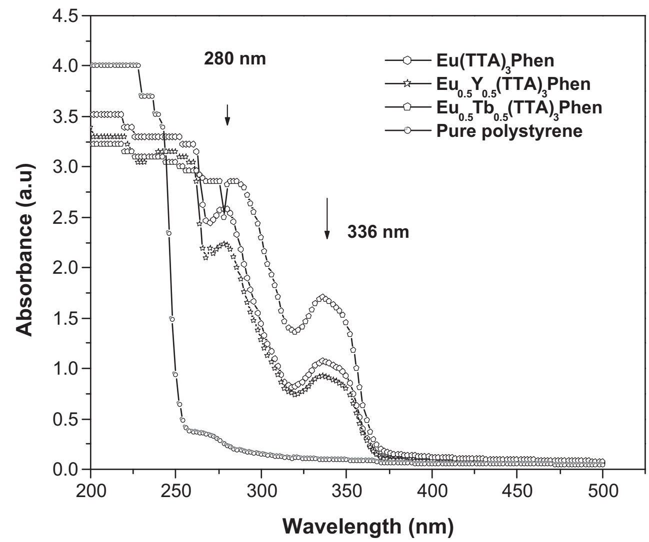


Fig. 19. Absorption spectra of $Eu(TTA)_3Phen$, $Eu_{0.5}$ $Y_{0.5}(TTA)_3Phen$ and $Eu_{0.5}$ $Tb_{0.5}(TTA)_3Phen$ blended films in PS.

taken as energy gap. The values obtained for energy gap (E_g) are 3.41, 3.35 and 3.43 eV for the blended films of $Eu(TTA)_3Phen$, $Eu_{0.5}Y_{0.5}(TTA)_3Phen$ and $Eu_{0.5}Tb_{0.5}(TTA)_3Phen$ in PMMA, respectively. Concentration effect on absorption and emission spectra was studied for different weight percentages (10, 25, 50, 60%). All the complexes doped in PMMA showed an excellent transparency of 90–97% while the complexes doped in polystyrene showed a transparency of 85–90%, which is bit less than in PMMA. Absorption peaks almost lied at same wavelength centered at 280 nm and 334 nm in PMMA; 280 nm and 336 nm in polystyrene, respectively with a change in optical density. Enhancement of emission intensity was observed when these complexes were doped in PMMA and PS, which is known as co-fluorescence. The luminescence intensity of blended films with 50 and 60% of rare earth complexes shows nearly equal intensity indicating that optimal doped concentration is not more than 50% under the chosen experimental conditions. Energy gap of $Eu(TTA)_3Phen$, $Eu_{0.5}Y_{0.5}(TTA)_3$ Phen and $Eu_{0.5}Tb_{0.5}(TTA)_3Phen$ have been determined in PMMA and PS. Hence, Eu(III) complexes are more compatible in polymer resins and exhibit enhancement in intensity when compared with the complexes in solid-state.

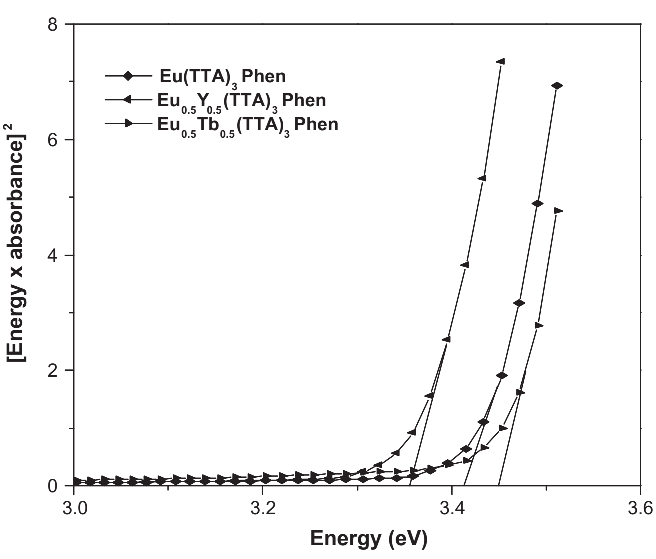


Fig. 18. Determination of energy gap of $Eu(TTA)_3Phen$, $Eu_{0.5}Y_{0.5}(TTA)_3Phen$ and $Eu_{0.5}Tb_{0.5}$ $(TTA)_3Phen$ in PMMA.

7.4.1. Polystyrene (PS)

Absorption spectra of $Eu(TTA)_3Phen$, $Eu_{0.5}Y_{0.5}(TTA)_3Phen$ and $Eu_{0.5}Tb_{0.5}(TTA)_3Phen$ blended film in PS at room temperature are shown in Fig. 19. Absorbance spectra of blended films in PMMA are characterized by two absorbance peaks centered at 336 nm and 280 nm. Usually, non-bonding orbital (n) with higher energy than pi anti bonding orbital (π^*) needs less amount of energy and hence observed at higher wavelength. At shorter wavelength, π–π^* transition is observed as this transition needs large amount of energy. The absorption peak λ_{max} at 334 nm is attributed to the non-bonding to pi anti bonding orbital (n–π^*) transition of β-diketonate ligand TTA while the other peak at 280 nm is attributed to π–π^* transition, which occurs from pi bonding orbital (HOMO) to pi anti bonding (LUMO) of the ligand in the europium complex. Among the three complexes doped in PS, $Eu_{0.5}Tb_{0.5}(TTA)_3Phen$ complex shows hyper chromic shift as compared to the remaining two complexes and hence better luminescent intensity can be expected in $Eu_{0.5}Tb_{0.5}(TTA)_3Phen$ than the other two. For all the doped complexes the absorption peak is at the same position because the ligand used is same in all the cases.

The values obtained in the determination of energy gap (E_g) for the blended films of $Eu(TTA)_3Phen$, $Eu_{0.5}Y_{0.5}(TTA)_3Phen$ and $Eu_{0.5}Tb_{0.5}(TTA)_3Phen$ in polystyrene are 3.35, 3.28 and 3.4 eV, respectively as shown in Fig. 20. Optical studies of the $Eu(TTA)_3Phen$, $Eu_{0.5}Y_{0.5}(TTA)_3Phen$ and $Eu_{0.5}Tb_{0.5}(TTA)_3Phen$ in polymer matrix were given Table 10.

7.5. Solvent effect on the optical properties of synthesized complexes

Solution-processable emissive compounds have attracted tremendous attentions during the past decades in organic light emitting diodes (OLEDs) field [170–175]. With respect to their polymer counter parts, solution-processable small molecules present the advantage of precise chemical structures and better reproducibility of synthesis, which facilitates the establishment of structural property relationship [176–178]. They offer the possibility of avoiding the troublesome high-precision mask alignment during vacuum deposition process. Based on the current

Table 10
Optical studies of the $Eu(TTA)_3Phen$, $Eu_{0.5}Y_{0.5}(TTA)_3Phen$ and $Eu_{0.5}Tb_{0.5}(TTA)_3Phen$ in polymer matrix.

Parameter	$Eu(TTA)_3$ Phen	$Eu_{0.5}Y_{0.5}(TTA)_3Phen$	$Eu_{0.5}Tb_{0.5}(TTA)_3Phen$
λ_{max} in PMMA (nm)	280, 334	280, 334	280, 334
λ_{max} in PS (nm)	280, 336	280, 336	280, 336
λ_{exci} in PMMA (nm)	381	387	380
λ_{exci} in PS (nm)	379	375	385
λ_{mi} in PMMA (nm)	611	611	611.4
λ_{emi} in PS (nm)	611	611	611.6
E_g in PMMA (eV)	3.41	3.35	3.43
E_g in PMMA (eV)	3.35	3.28	3.4

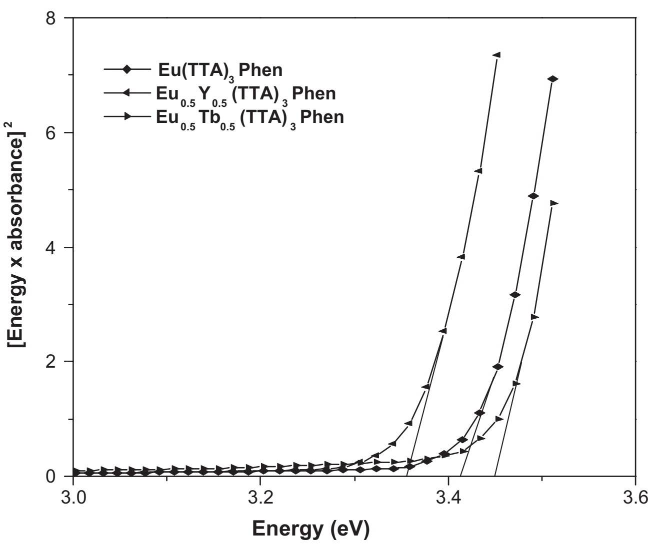


Fig. 20. Determination of energy gap of $Eu(TTA)_3Phen$, $Eu_{0.5}Y_{0.5}(TTA)_3Phen$ and $Eu_{0.5}Tb_{0.5}(TTA)_3Phen$ in PS.

development of OLED materials [179–181], the design and synthesis of efficient non-doped red emitter with facile synthesis and purification method, good processability, efficient electron injection/transport capability and saturated red emission still remain the key issue [182–187].

As organic materials are soluble in different solvents, desired thickness can be deposited on the substrate by spraying these solvated organic complexes by solution techniques which is much simpler than vacuum deposition technique [188]. With time, the solvent evaporates and a film of organic layer can be obtained with ease. The choice of solvent is significant as the emission intensity in that particular solvent depends upon the absorption spectra of the solvated complex. Considering these facts, the absorption spectra of $Eu(TTA)_3Phen$, $Eu_{0.5}Y_{0.5}(TTA)_3Phen$ and $Eu_{0.5}Tb_{0.5}(TTA)_3Phen$ complexes are studied in different solvents. The advantage of these organic complexes is that they are soluble in most of the organic solvents as well as in some acidic medium, offering a path to study the absorption as well as emission spectra in different solvents with different molar ratios. In the present work, the shift of π–$\pi^*$and n–π^* transitions in the absorption spectra of $Eu(TTA)_3Phen$, $Eu_{0.5}Y_{0.5}(TTA)_3$ Phen and $Eu_{0.5}Tb_{0.5}(TTA)_3Phen$ complexes in different solvent media was studied. Optical energy band gap of these complexes in different solvents is also calculated. Basic organic solvents (chloroform, toluene, tetra hydro furan) and acidic solvents (acetic acid and formic acid) were used in the present study.

The impact of solvent on the optical absorption properties of $Eu(TTA)_3Phen$, $Eu_{0.5}Y_{0.5}(TTA)_3$ Phen and $Eu_{0.5}Tb_{0.5}(TTA)_3Phen$ organic luminescent complexes was studied These complexes can be made into thin films by solution processing technique as they show good solubility in most of the solvents including chloroform, toluene, tetra hydro furan, carbon tetra chloride, acetic acid, formic acid, etc. Optical absorption spectra of these complexes were carried out in different solvents with different molar ratios. Absorption peaks of these complexes in basic media are clearly at shorter wavelengths than in acidic media. Energy gap of these complexes were determined in different solvents for 10^{-4} M ratio. These complexes show different absorption wavelength λ_{max} in different solvents, reflecting the impact of the solvent on absorption properties of organic luminescent complexes. Optical absorption spectra in solvated $Eu(TTA)_3Phen$, $Eu_{0.5}Y_{0.5}(TTA)_3Phen$ and $Eu_{0.5}Tb_{0.5}(TTA)_3Phen$ complexes are shown in Table 11.

7.6. Fabrication of OLED devices

OLED devices having the structure ITO/m-MTDATA/α-NPD/TPBi: $Eu_{(x)}Y_{(1-x)}(TTA)_3Phen/Alq_3$/LiF:Al (where x = 0.4, 0.5) were fabricated on Doosan DND OLED fabrication system by vacuum deposition technique [189–192]. Structure of fabricated OLED devices is shown in Fig. 21. An ITO glass substrate coated with patterned indium tin oxide (ITO) with sheet resistance less than 10 ohm/square is taken as base for the deposition of organic layers. This ITO is a transparent and conductive glass substrate with high work function ($\varphi_W \approx 4.7$–4.9 eV). ITO glass plate is itched, patterned and carefully cleaned under low-pressure plasma before deposition. ITO glass plate is pre-heated with the flow of plasma (oxygen and argon) at a rate of 50 SCCM at a pressure of 80 mTorr. This ITO is placed on a holder and then transferred to plasma chamber from the glove box for plasma treatment. This ITO glass plate is used as base and the organic layers are successfully deposited at a pressure of 6×10^{-8} Torr in a vacuum system consisting of two connected vacuum chambers namely organic chamber and metal chamber. In one chamber organic layers are deposited by vacuum deposition with base pressure of 6×10^{-8} Torr utilizing the deposition rate of 1 Å/s. The thickness of HIL, HTL, EML: dopant (15 wt%), ETL are 1000, 200, 250, 250 Å, respectively. The sample is transferred from organic chamber to the metal chamber without breaking the vacuum. An hole injecting material m-MTDATA(4,4′,4″tris (3methylphenylpheny lamino) triphenylamine) helps to balance hole and electron injection. The thickness of the HIL needs to be thick enough to planarize or wet the surface of the anode layer. However, since anode surfaces tend to be very rough, a thickness of up to 1000 Å may be desired for HIL in some cases. m-MTDATA has been identified as effective material in promoting injection of holes from ITO into hole transporting layers (HTL) with a hole mobility of about 3×10^{-5} cm^2. HTL is selected such that the HOMO and LUMO levels lie in midway between hole injection layer and electron transport layer. As α-NPD satisfies the requirement, it is selected as HTL layer in the present study. As Eu complexes doped with appropriate host exhibit high efficiency, $Eu_{(x)}Y_{(1-x)}(TTA)_3Phen$ doped with TPBi(1,3,5-tris(N-Phenylbenzimidizol-2-yl)) benzene host at 15 wt% is used as emissive layer. The host electron transporting material in the ETL is selected such that electrons can be efficiently injected from the cathode into the LUMO level of the electron transporting material. Alq_3 exhibit highly stable film

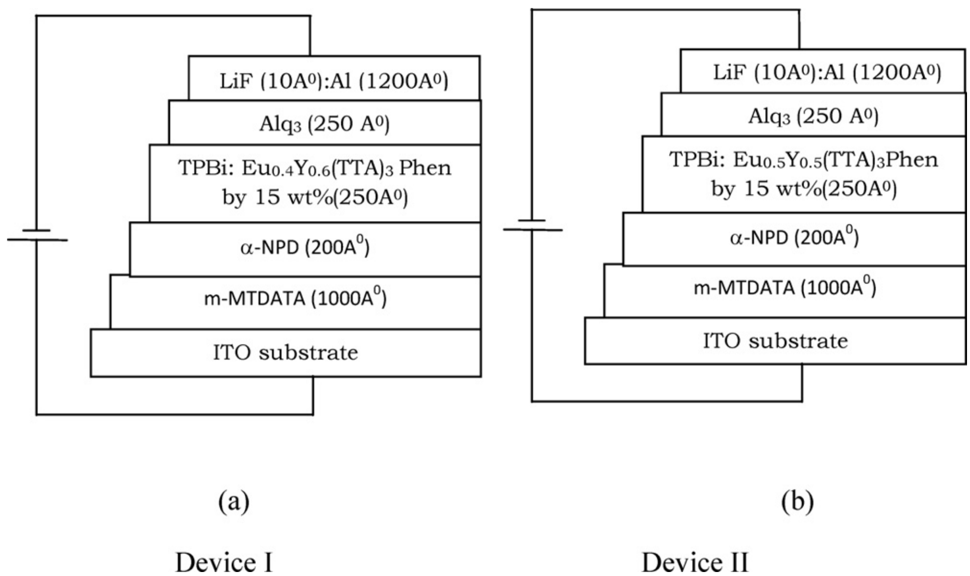


Fig. 21. Structure of fabricated OLED devices.

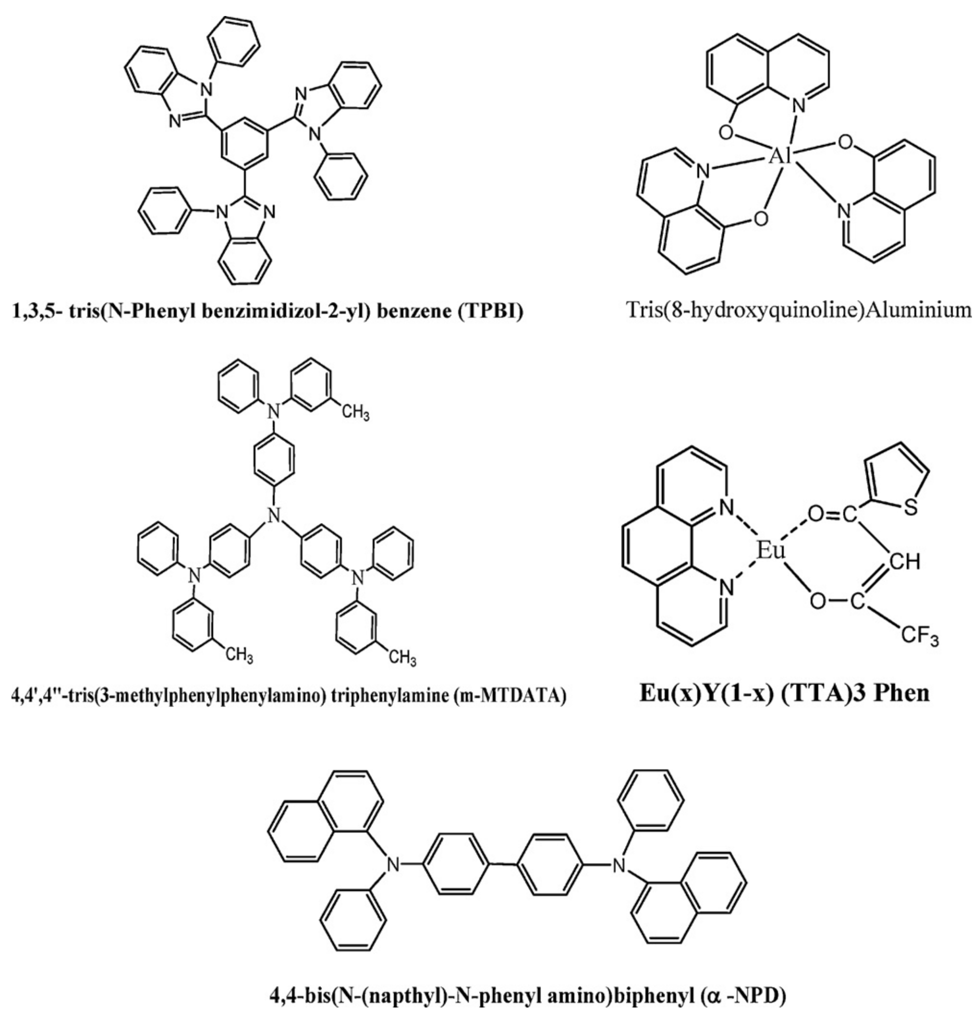


Fig. 22. Molecular structure of the materials used in fabricating OLED devices.

forming characteristics, good carrier transport properties and good heat resistance and hence chosen as a model ETL. Electron hole transporting layers play a vital role on the EL device performance. Electron injection from Al cathode to the electron transport layer is enhanced by a thin LiF buffer layer and hole injection from ITO anode to HTL, there by the injection of electrons and holes in the emissive layer will be greatly enhanced. Finally, in the metal chamber, LiF buffer layer and aluminum cathode (LiF 10 Å:Al

Table 11
Optical absorption spectra in solvated Eu(TTA)$_3$Phen, Eu$_{0.5}$Y$_{0.5}$(TTA)$_3$Phen and Eu$_{0.5}$Tb$_{0.5}$(TTA)$_3$Phen complexes.

Parameter	Eu(TTA)$_3$Phen	Eu$_{0.5}$Y$_{0.5}$(TTA)$_3$Phen	Eu$_{0.5}$Tb$_{0.5}$(TTA)$_3$Phen
λ_{max} in chloroform (nm)	261, 331	261, 329	261, 329
λ_{max} in toluene (nm)	329	329	329
λ_{max} in THF (nm)	260, 330	271, 331	265, 331
λ_{max} in acetic acid (nm)	261, 344	263, 310	261, 344
λ_{max} in formic acid (nm)	271, 346	263, 347	271, 346
E_g in chloroform (eV)	3.42	3.43	3.42
E_g in toulene (eV)	3.41	3.42	3.41
E_g in THF (eV)	3.39	3.41	3.39
E_g in acetic acid (eV)	3.38	3.36	3.34
E_g in formic acid (eV)	3.35	3.29	3.28

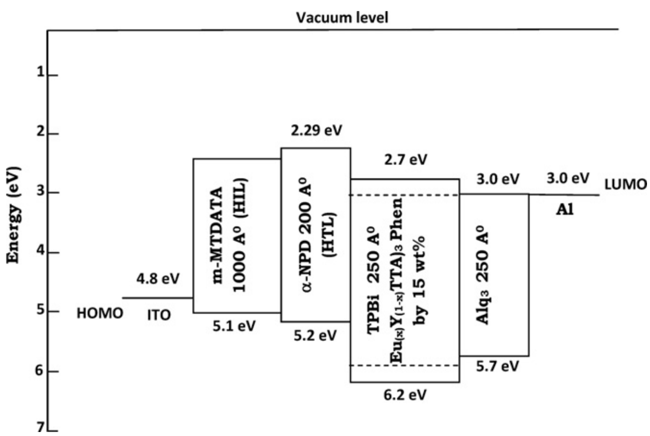


Fig. 23. The band structure of device I and device II.

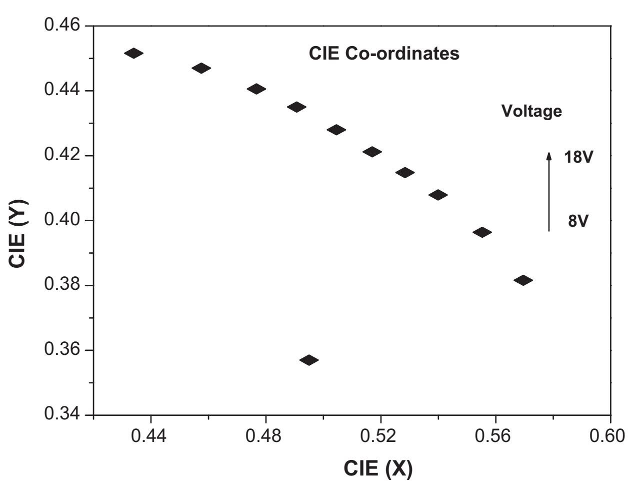


Fig. 24. CIE coordinates of Eu$_{0.4}$Y$_{0.6}$(TTA)$_3$Phen OLED devices.

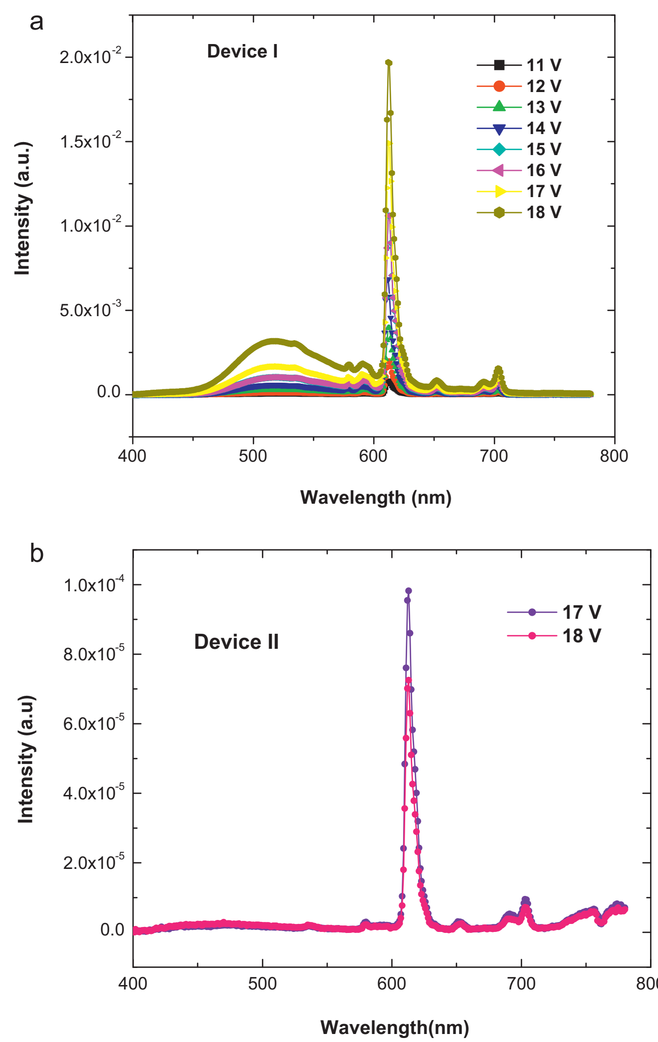


Fig. 25. Electroluminescence (EL) spectra of (a) device I and (b) device II.

1500 Å) were deposited at a base pressure of 6×10^{-8} Torr, utilizing the deposition rate of 0.01 Å/s and 2 Å/s, respectively. As both low work function cathode and organic materials are sensitive to oxygen and moisture, the devices are encapsulated using a glass lid sealed to the substrate with a bead of UV cured epoxy in a nitrogen filled glove box (dew point ≈ 75 °C) for 3 min after fabrication. The molecular structure of the materials used and the band structure of OLED devices are illustrated in Figs. 22 and 23 respectively.

7.7. Characterization of OLED devices

7.7.1. CIE coordinates

Color coordinates (CIE: Internationale de I' Eclairage) of the emitting light from device I are graphically shown in Fig. 24. It can be observed that with the increasing bias voltage the color coordinates shifted towards shorter wavelength.

7.7.2. Electroluminescence spectra

EL spectra of device I and device II for 16 mm^2 device area is shown in Fig. 25(a) and (b), respectively at different bias voltage. Maximum luminance of 187.6 cd/m^2 and 47.72 cd/m^2 is achieved at 612 nm for device I and device II, respectively at a bias voltage of 18 V. The spectra contain five primary peaks at 525, 590, 612, 650, 704 nm, corresponding to $^5D_0 \rightarrow {}^7F_j$ transitions (j = 0, 1, 2, 3, 4). The sharp emission peak at 612 nm is due to electric dipole induced $^5D_0 \rightarrow {}^7F_2$ transition. The observed Eu^{3+} emission is due to the long

lifetime of $^5D_0$ state. Due to this long lifetime this state can be easily filled very quickly and the emission accordingly saturates [193]. OLED devices are fabricated using $Eu_{(x)}Y_{(1-x)}(TTA)_3$Phen organic luminescent complexes (x = 0.4, 0.5) as the organic emissive layer by vacuum deposition technique. Various characterization techniques such as I–V, J–V–L, V–L characteristics, CIE co-ordinates and electroluminescence (EL) spectra were carried out for the fabricated devices. Turn on voltage of OLED device I and device II was found to be 13 V and 17 V, respectively. Intense red emission was observed for both the devices at 612 nm when operated in a range of 10–18 V. Maximum brightness of 186.5 cd/m^2 and 44.72 cd/m^2 was observed for device I and device II, respectively when operated at 18 V, suggesting potential application in various displays and electro-optical devices.

8. Conclusions

Review on OLEDs and its materials reveals that electricity to light conversion efficiency, device stability and life time, especially blue color, material selection and optimization, encapsulation to prevent device from water, oxygen and any reacting chemical, uniformity over large areas, manufacture cost, especially for large area, fine patterning, contrast, pixel switching, color saturation are the challenges presently ahead in order to compete with the present lighting system with the eco-friendly OLEDs. Significant efforts have been made at global level on development and fabrication of red, green and blue emitting complexes and devices. However, further improvements in efficiency are required to take over a large proportion of the flat panel display market. OLEDs can maintain the same level of luminance at much lower voltage and current levels, significantly reducing the energy consumption and operation costs. Reduced energy needs increases lifespan of OLEDs by more than four times, making these devices more cost-effective and affordable in long-term projections. A fourfold increase in light extraction efficiency does not affect internal efficiency, allowing the OLED to maintain extremely high internal efficiency levels while simultaneously improving external efficiency. This light extraction mechanism can be included in current manufacturing processes, saving time and money by utilizing existing device fabrication techniques decreased energy consumption significantly decreases the environmental impact of owning and operating OLEDs.

After peer review of literature, we have reported the synthesis and characterization of Eu(III) activated red light emitting materials, fabrication and characterization of OLED devices using $Eu_{(x)}Y_{(1-x)}(TTA)_3$Phen complexes. The conclusions from the above studies are as follows.

XRD measurements reveal the crystalline nature of all the synthesized complexes. Thermal stability was found to be improved in binuclear Eu complexes $Eu_{(x)}Y_{(1-x)}(TTA)_3$Phen, and $Eu_{(x)}Tb_{(1-x)}(TTA)_3$Phen (where x = 0.4 and 0.5) than in pure $Eu(TTA)_3$Phen complex. Among all the synthesized complexes, $Eu_{0.4}Tb_{0.6}(TTA)_3$Phen shows maximum thermal stability. Melting point of binuclear complexes is at higher value than the melting point of pure $Eu(TTA)_3$Phen complex. Among all the synthesized complexes, $Eu_{0.5}Tb_{0.5}(TTA)_3$Phen shows higher melting point. Intense red emission at 611 nm was found to be more in binuclear Eu complexes than in pure Eu complexes. All the three complexes doped in PMMA shows good transparency than in polystyrene. $Eu_{0.5}Tb_{0.5}(TTA)_3$Phen complex shows good optical density in the absorption spectra when compared with the other complexes in PMMA and PS.$Eu_{0.5}Tb_{0.5}(TTA)_3$Phen complex shows good optical density in the absorption spectra in PMMA than in PS. The blended films of $Eu(TTA)_3$Phen, $Eu_{0.5}Y_{0.5}(TTA)_3$Phen, and $Eu_{0.5}Tb_{0.5}(TTA)_3$Phen organic luminescent complexes in PMMA/PS show enhancement in fluorescence intensity. The emission intensity of the doped complexes increased by the order of twofolds in PMMA and of the order of more than onefold in polystyrene. Among the three complexes in PMMA and PS, $Eu_{0.5}Tb_{0.5}(TTA)_3$Phen complex show maximum luminescent intensity. Among the all wt% considered, the complexes with wt% of 50% shows maximum luminescent intensity. Energy gap of $Eu(TTA)_3$Phen, $Eu_{0.5}Y_{0.5}(TTA)_3$Phen, and $Eu_{0.5}Tb_{0.5}(TTA)_3$Phen complexes in PMMA is found to be 3.41, 3.35 and 3.43 eV, respectively. Energy gap of $Eu(TTA)_3$Phen, $Eu_{0.5}Y_{0.5}(TTA)_3$Phen, and $Eu_{0.5}Tb_{0.5}(TTA)_3$Phen complexes in Polystyrene is found to be 3.35, 3.28 and 3.4 eV, respectively. λ_{max} of $Eu(TTA)_3$Phen, $Eu_{0.5}Y_{0.5}(TTA)_3$Phen and $Eu_{0.5}Tb_{0.5}(TTA)_3$ Phen complexes shifts to a different value with the change in solvent. λ_{max} of $Eu(TTA)_3$Phen, $Eu_{0.5}Y_{0.5}(TTA)_3$Phen, and $Eu_{0.5}Tb_{0.5}$ $(TTA)_3$ Phen complexes for different molar ratios remained unaltered for a particular solvent. λ_{max} of $Eu(TTA)_3$Phen, $Eu_{0.5}Y_{0.5}(TTA)_3$Phen, and $Eu_{0.5}Tb_{0.5}(TTA)_3$ Phen complexes was found to be more in acidic media than in basic media. Red organic light emitting diode (OLED) devices were fabricated using binuclear $Eu_{(x)}Y_{(1-x)}(TTA)_3$Phen organic luminescent complexes. Device I made of $Eu_{0.4}Y_{0.6}(TTA)_3$Phen showed better performance than device II made of $Eu_{0.5}Y_{0.5}(TTA)_3$Phen. Turn on voltage of device I and device II found to be 13 V and 17 V, respectively. Maximum brightness of 186.5 cd/m^2 and 44.72 cd/m^2 is observed for device I and device II, respectively when operated at 18 V. Significant red emission is observed from fabricated OLED devices at 612 nm when operated in a range of 10 to 18 V.Although the driving voltage is rather high compared to the other OLED devices, the device performance can be improved by employing highly purified organic complexes, implementing the method of co-doping controlling the thickness of each layer, proper selection of HIL, HTL, ETL as well as the device structure. Emission color is basically determined by the energy difference of HOMO and LUMO of the emitting organic material. Consequently by changing these active materials the emission color can be varied across the visible spectrum.

To compete with LCDs, both OLED small molecule and polymer technologies must combine high resolution and full color with highly competitive production costs. Recently a production process that enables RGB (red-green-blue) deposition at high resolution, using a photolithographic technique has been developed. This process exploits a new class of electroluminescent polymers that can be spin-coated and cured by ultraviolet light, but maintain their electrical and optical properties. Combined with a simple patterning process, the development enables the creation of high-resolution pixelated matrix displays. This new production technology overcomes the resolution limitations encountered in previous fabrication techniques, such as ink-jet deposition. Instead, it uses standard photolithography that is well established in the volume production of many electronic components, such as color filters for LCD monitors. When fully commercialized, it promises to combine the high performance and competitively lower costs of PLEDs with a higher resolution. Perhaps the most exciting future development to look forward to is the flexible “all-plastic” display, an OLED display that combines a plastic substrate with organic polymer electronics.

References

[1] McGehee MD, Bergstedt T, Zhang C, Saab AP, O'Regan MB, Bazan GC, et al. Adv Mater 1999;11:1346.
[2] Zhao D, Hong Z, Liang C, Zhao D, Liu X, Li W, et al. Thin Solid Films 2000;363:208.
[3] Liang CJ, Hong ZR, Liu XY, Zhao DX, Zhao D, Li WL, et al. Thin Solid Films 2000;14:359.
[4] Pyo SW, Lee SP, Lee HS, Kwon OK, Hoe HS, Lee SH, et al. Thin Solid Films 2000;232:363.
[5] Zhu W, Jiang Q, Lu Z, Wei X, Xie M, Zou D, et al. Synth Met 2000;445:111–2.
[6] Zhao D, Li W, Hong Z, Liu X, Liang C, Zhao D. J Lumin 1999;82:105.

[7] Jensen WB. J Chem Educ 2003;80(8):952–61.
[8] Figgis BN, Lewis J, Lewis J, Wilkins RG, editors. The magnetochemistry of complex compounds. Modern coordination chemistry. New York: Interscience; 1960. p. 400–54.
[9] Matsumoto PS. J Chem Educ 2005;82:1660.
[10] Dunn TM. In: Lewis J, Wilkins RG, editors. Modern Co-ordination Chemistry, vol. 4. New York: Interscience; 1960. p. 268–73. Chapter.
[11] Kido J, Nagai K, Okamoto Y. J Alloys Compd 1993;192:30.
[12] Kido J, Nagai K, Okamoto Y, Skotheim T. Chem Lett 1991;235:1267.
[13] Zhang X, Sun R, Zheng Q, Kobayashi T, Li W. Appl Phys Lett 1997;71:2596.
[14] Hong Z, Li W, Zhao D, Liang C, Liu X, Peng J, et al. Synth Met 1995;104:165.
[15] Whan RE, Crosby GA. J Mol Spectrosc 1962;8:315.
[16] Bhaumik ML, El-Sayed MA. J Chem Phys 1965;42:787.
[17] Huang HG, Hiraki K, Nishikawa Y. Nippon Kagaku Kaishi (Internal Report) 1981;1:66.
[18] Rikken GLJA. Phys Rev A 1995;51:4906.
[19] Ashcroft NW, Mermin ND. Solid State Physics. Philadelphia: Saunders; 1976.
[20] Gschneiduer Jr KA, Bünzli JCG, Pencharsky VK, editors. Hand book on physics and chemistry of Rare earth, vol. 35. Elsevier; 2005.
[21] Kadarkaraisamy M, Sykes AG. Inorg Chem 2006;45(2):779–86.
[22] Lee H, Choi S-H. J Appl Phys 1999;85(3):1771–4.
[23] Wakimoto T, Murayama R, Nagayama K, Okuda Y, Nakada H, Tohma T. SID Int Symp Digest 1996;849.
[24] http://electronics.howstuffworks.com.
[25] Kido J, Ikeda W, Kaimura M, Nagai K. Jpn J Appl Phys 1996;35:L394.
[26] Peters MG, High power, high efficiency diode lasers at JDSU, Talk PTuC3, Program of the conference on lasers and electro-optics conference, May 21–26; 2006. p. 14, http://www.cleoconference.org/materials/CLEO06TuesdayWeb5.pdf.
[27] Ohno Y. Optical metrology for LEDs and solid state lighting. Proc SPIE 2006;6046:604625.
[28] Zhmakin AI. Phys Rep 2011;498:189–241.
[29] Tang CW, VanSlyke SA. Appl Phys Lett 1987;51:913.
[30] Kido J, Nagai M, Ohashi Y. Chem Lett 1990;13:657.
[31] Biltz W. Ann 1904;331:334.
[32] Jantzch G, Meyer E. Ber 1920;53:577.
[33] Van Uitert LG, Soden RR. In: Kirseliner S, editor. Advances in the chemistry of coordination compounds. New York, NY: The Macmillan Co.; 1961. p. 613.
[34] Moeller T, Horwitz EP. J Inorg Nucl Chem 1959;12:49.
[35] Pope M, Kallamann HP, Magnante P. J Chem Phys 1963;38:2042.
[36] Brock EG, Csavinsky P, Hormats E, Neddermann HC, Strip D, Unterleittner F. J Chem Phys 1961;35:759.
[37] Lempicki A, Samelson H. Phys Lett 1963;2:133.
[38] Hart FA, Laming FP. Proc Chem Soc 1963;107.
[39] Levine AK, Palilla FC. Appl Phys Lett 1964;5:118.
[40] Ohlmann RC, Charles RG. J Chem Phys 1964;40:3131.
[41] Melby LR, Roze NR, Abramson E, Caris JC. Am J Chem Soc 1964;86:5117.
[42] Dresner J. RCA Rev 1969;30:322.
[43] Gold H. In: Venkataraman K, editor. The chemistry of synthetic dyes, vol. 5. New York: Academic; 1971. p. 535.
[44] Drexhage KH. In: Schafer FP, editor. Topics in applied physics: dye lasers, vol. 1. New York: Springer; 1977. p. 144.
[45] Kampas FJ, Gouterman M. Chem Phys Lett 1977;48:233.
[46] Bryant FJ, Krier A. Phys Status Solidi A 1984;81:681.
[47] Kalinowski J, Godlewski J, Dreger Z. Appl Phys A 1985;37:179.
[48] Koezuka H, Tsumura A, Ando Y. Synth Met 1987;18:69.
[49] Horowitz G, Fichou D, Peng XZ, Xu Z, Garnier F. Solid State Commun 1989;729:381.
[50] Burroughes JH, Bradley DDC, Brown AR, Marks RN, Mackayr K, Friend H, et al. Nature 1990;347:539.
[51] Brittain HG. J Coord Chem 1990;21:295.
[52] Li W, Li WL, Tang MD, Chin J. Rare Earth Soc 1989;7:27.
[53] Li W, Li W, Yu G, Wang Q, Jin R. J Alloys Compd 1993;192:34.
[54] Kido J, Hayase H, Hongawa K, Nagai K, Okuyama K. Appl Phys Lett 1994;65:17.
[55] Li W, Li W, Yu G, Wang Q, Jin R. J Alloys Compd 1993;192:34–6.
[56] Sano T, Fujita M, Fujii T, Hamada Y, Shibata K, Kuroki K. Jpn J Appl Phys 1995;34:1883.
[57] Rodritguez–Ubis JC, Alonso MT, Juanes O, Sedano R, Brunet E. J Lumin 1998;79:121.
[58] Uekawa M, Miyamoto Y, Ikeda H, Kaifu K, Nakaya T. Synth Met 1997;91:259.
[59] Wang M, Qian G, Lii S. Mater Sci Eng B 1998;55:119.
[60] Hao X, Fan X, Wang M. Thin Solid Films 1999;353:223.
[61] Miyamoto Y, Uekawa M, Ikeda H, Kaifu K. J Lumin 1999;81:159.
[62] Fu L, Zhang H, Wang S, Meng Q, Yang K, Ni J. J Sol Gel Sci Technol 1999;15:49.
[63] Meng Q, Zhang H, Wang S, Fu L, Zheng Y, Yang K. Mater Lett 2000;45:213.
[64] Zheng Y, Shi C, Liang Y, Lin Q, Guo C, Zhang H. Synth Met 2000;114:321.
[65] Heil H, Steiger J, Schmechel R, Von Segger H. J Appl Phys 2001;90:5357.
[66] Tsaryuk V, Zolin V, Legendziewicz J, Sokolnicki J, Kndryashova V.Proc. of EL 2002. 2002. p. 165.
[67] Kim JS, Jeon PE, Choi JC, Park HL. Appl Phys Lett 2004;84(15):2931–3.
[68] Wang H, Wang R, Sun X, Yan R, Li Y. Mater Res Bull 2005;40:911–9.
[69] Yang H-M, Shi J-X, Liang H-B, Gong M-L. Mater Res Bull 2006;41:867–72.
[70] Lee C, Lim JS, Kim SH, Suh DH. J Polym 2006;47(15):5253–8.
[71] Całus S, GondekF E., Danel A, Jarosz B, Nizioł J, Kityk AV. Mater Sci Eng B 2007;137:255–62.
[72] Park GY, Ha Y. Synth Met 2008;158:120–4.
[73] Collins AM, Olof SN, Mitchels JM, Mann S. J Mater Chem 2009;19:3950–4.
[74] Seo JH, Lee SC, Kim YK, Kim YS. Thin Solid Films 2009;517:4119–21.
[75] Shukla P, Sudarsan V, Vatsa RK, Nayak SK, Chattopadhyay S. J Lumin 2010;130:1952–7.
[76] Nandhikonda P, Heagy MD. Chem Commun 2010;46:8002–4.
[77] Thejo Kalyani N, Dhoble SJ, Ahn JS, Pode RB. J Korean Phys Soc 2010;57(4):746–51.
[78] Belian MF, Freire RO, Galembeck A, deSaĩ GF, deFarias RF, Alves Jr S. J Lumin 2010;130:1946–51.
[79] Tao S, Jiang Y, Lai S-L, Fung M-K, Zhou Y, Zhang X, et al. Org Electron 2011;12:358–63.
[80] Li G. J Lumin 2011;131:184–9.
[81] Hu B, Zhang J, Chen Y. Eur Polym J 2011;47:208–24.
[82] Tang H, Li Y, Wei C, Chen B, Yang W, Wu H, et al. Dyes Pigments 2011;91:413–21.
[83] Gschneiduer Jr KA, Bünzli JCG, Pencharsky VK, editors. Hand book on physics and chemistry of Rare earth, vol. 35. Elsevier; 2005.
[84] de Mello Donegá C, Alves Jr S, de Sá GF. J Alloys Compd 1997;250:422.
[85] Malta OL, Brito HF, Menezes JFS, Gonçalves e Silva FR, Alves Jr S, Farias Jr FS, et al. J Lumin 1997;75:255.
[86] Qian GD, Wang MQ, Yang Z. J Non-Cryst Solids 2001;286:235.
[87] Bünzli JCG, Moret E, Foiret V, Schenk KJ, Wang MZ, Jin LP. J Alloys Compd 1994;107:207–8.
[88] Alves Jr S, Almeida FV, de Sá GF, de MelloDonegá C. J Lumin 1997;478:72–4.
[89] Gonçalves e Silva FR, Menezes JFS, Rocha GB, Alves S, Brito HF, Longo RL, et al. J Alloys Compd 2000;364:303–4.
[90] Brito HF, Malta OL, Menezes JFS. J Alloys Compd 2000;336:303–4.
[91] Malandrino G, Bettinelli M, Speghini A, Fragala IL. Eur J Inorg Chem 2001;1039.
[92] Yan B, Zhang HJ, Wang SBJ, Ni Z. Mater Chem Phys 1997;51:92.
[93] Liss IB, Bos WG. J Inorg Nucl Chem 1977;39:443.
[94] Kononenko LI, Melent'eva EV, Vitkun RA, Poluektov NS. Ukr Khim Zh 1965;31:1031.
[95] Liang CY, Schimitschek EJ, Trias JA. J Inorg Nucl Chem 1970;32:811.
[96] Melby LR, Rose NJ, Abramson E, Caris JC. J Am Chem Soc 1964;86:5117.
[97] Bauer H, Blanc J, Ross DL. J Am Chem Soc 1964;86:5125.
[98] Charles RG, Riedel EP. J Inorg Nucl Chem 1966;28:3005.
[99] Batista HJ, de Andrade AVM, Longo RL, Simas AM, de Sá GF, Ito NK, et al. Inorg Chem 1998;37:3542.
[100] Anonymous, H.W. Sands Corp. http://www.hwsands.com/index.html; 2004.
[101] Van Meervelt L, Froyen A, D'Olieslager W, Walrand-Görller C, Drisque I, King GSD, et al. Bull Soc Chim Belg 1996;105:377.
[102] Charles RG. Inorg Synth 1967;9:37.
[103] Butter E, Kreher K. Z Naturforsch A 1965;20:408.
[104] Charles RG, Ohlmann RC. J Inorg Nucl Chem 1965;27:119.
[105] Wang KZ, Huang L, Gao LH, Huang CH, Jin LP. Solid State Commun 2002;122:233.
[106] Moser DF, Thompson LC, Young Jr VG. J Alloys Compd 2000;121:303–4.
[107] Springer Jr CS, Meek DW, Sievers RE. Inorg Chem 1967;6:1105.
[108] Mattson SM, Abramson EJ, Thompson LC. J Less-Common Met 1985;112:373.
[109] Iftikhar K, Sayeed M, Ahmad N. Inorg Chem 1982;21:80.
[110] Berg EW, Acosta JJC. Anal Chim Acta 1968;40:101.
[111] Halverson F, Brinen JS, Leto JR. J Chem Phys 1964;40:2790.
[112] Bhaumik ML. J Inorg Nucl Chem 1965;27:243;
Bhaumik ML. J Inorg Nucl Chem 1965;27:261.
[113] Hellmuth K-H, Mirzai H, Fresenius Z. Anal Chem 1985;321:124.
[114] Thompson LC, Berry S. J Alloys Compd 2001;177:323–4.
[115] Shigematsu T, Matsui M, Utsunomiya K. Bull Chem Soc Jpn 1969;42:1278.
[116] Leedham TJ, Drake SR, US Patent 5,504 (1996) 195.
[117] Malta OL, Couto dos Santos MA, Thompson LC, Ito NK. J Lumin 1996;69:77.
[118] Selbin J, Ahmad N, Bhacca N. Inorg Chem 1971;10:1383.
[119] Ansari MS, Ahmad N. J Inorg Nucl Chem 1975;37:2099.
[120] Utsunomiya K. Anal Chim Acta 1972;59:147.
[121] Purushottam D, Ramachandra Rao V, Raghava Rao BSV. Indian J Chem 1965;33:182.
[122] Wang KZ, Gao LH, Huang CH. J Photochem Photobiol A 2003;156:39.
[123] Halls JJM, Arias AC, MacKenzie JD, Wu W, Inbasekaran M, Woo EP, et al. Adv Mater 2000;12:498.
[124] Xia Y, Friend RH. Adv Mater 2006;18:1371.
[125] Grimsdale AC, Cahn KL, Martin RE, Jokisz PG, Holmes AB. Chem Rev 2009;109:897–1091.
[126] Huang JL, Wu GE, Xu Q, Yang Y. Adv Mater 2006;18:114–7.
[127] Dailey S, Feast WJ, Peace RJ, Sage IC, Tilla S, Wooda EL. J Mater Chem 2001;11:2238.
[128] Hu J, Zhao H, Zhang Q, He W. J Appl Polym Sci 2003;89:1124–31.
[129] Liu HG, Lee Y, Park S, Jang K, Kim SS. J Lumin 2004;110(1–2):11–6.
[130] Liu HG, Park S, Jang K, Feng XS, Kim C, Seo HJ, et al. J Lumin 2004;106(1):47–55.
[131] Jiu H, Ding J, Sun Y, Bao J, Gao C, Zhang Q. J Non-Cryst Solids 2006;352(3):197–202.
[132] Kido J, Nagai K. J Alloys Compd 1993;192:30–3.
[133] Adachi C, Baldo MA, Forest SR. J Appl Phys 2000;87:11.
[134] Chen B, Lin X, Cheng L, Lee C, Gambling WA, Lee S. J Phys D: Appl Phys 2001;34:30–5.
[135] Ma C, Zhang B, Liang Z, Xie P, Wang X, Zhang B, et al. J Mater Chem 2002;12:1671–5.

[136] Ohmari Y, Kajii H, Sawatani T, Ueta H, Yoshino K. J Curr Appl Phys 2005;5(4):345–7.
[137] Qu B, Chen Z, Liu Y, Cao H, Xu S, Cao S, et al. J Phys D: Appl Phys 2006;39:2680–3.
[138] Ni SY, Wang XR, Wu YZ, Chen HY, Zhu WQ, Jiang XY, et al. Appl Phys Lett 2004;85(6).
[139] Gondek E, Kityk IV, Danel A, Wisla A, Sanetra J. Synth Met 2006;156:1348–54.
[140] Xu M, Zhou R, Wang G, Yu J. Inorg Chim Acta 2009;362:2183–8.
[141] Khizar-ul-Haq, Khan MA, Jiang XY, Zhang ZL, Zhang XW, Wei B, et al. J Lumin 2009;129:1158–62.
[142] Khizar-ul Haq, Liu SP, Khan MA, Jiang XY, Zhang ZL, Cao J, et al. Curr Appl Phys 2009;9:257–62.
[143] Wu C-H, Chien C-H, Hsu F-M, Shih P-I, Shu C-F. J Mater Chem 2009;19:1464–70.
[144] Park Y, Seok C-H, Lee J-H, Park J. Synth Met 2010;160:845–8.
[145] Wettach H, Jester SS, Colsmann A, Lemmer U, Rehmann N, Meerholz K, et al. Synth Met 2010;160:691–700.
[146] Cho MJ, Jin J-I, Choi DH, Yoon JH, Hong CS, Kim YM, et al. Dyes Pigments 2010;85:143–51.
[147] Zhang Y, Xie C, Su H, Liu J, Pickering S, Wang Y, et al. Nano Lett 2011;11:329–32.
[148] Xie J, Chen C, Chen S, Yang Y, Shao M, Guo X, et al. Org Electron 2011;12:322–8.
[149] Kim S-J, Zhang Y, Zuniga C, Barlow S, Marder SR, Kippelen B. Org Electron 2011;12:492–6.
[150] Thejo Kalyani N, Dhoble SJ, Pode RB. Adv Mater Lett 2011;2(1):65–70.
[151] Seo JH, Lee SJ, Seo BM, Moon SJ, Lee KH, Park JK. Org Electron 2010;11:1759–66.
[152] D'Andrade BW, Forrest SR. Adv Mater 2004;16:1585–95.
[153] Seo JH, Park JH, Kim YK, Kim JH, Hyung GW, Lee KH. Appl Phys Lett 2007;90(203):507–9.
[154] Yook KS, Lee JY. Appl Phys Lett 2008;92(193):308–10.
[155] Tong QX, Lai SL, Chan MY, Tang JX, Kwong HL, Lee CS. Appl Phys Lett 2007;91(023):503–5.
[156] Ho MH, Hsu SF, Ma JW, Hwang SW, Yeh PC, Chen CH. Appl Phys Lett 2007;91:113518.
[157] Sun Y, Forrest SR. Appl Phys Lett 2007;91(263):503–5.
[158] Wang Y, Liu Y, Zhang Z, Luo J, Shi D, Tan H, et al. Dyes Pigments 2011;91:495–500.
[159] Pimputkar S, Speck JS, Den Baars SP, Nakamura S. Nat Photon 2009;3:180–5.
[160] Ye S, Xiao F, Pan YX, Ma YY, Zhang QY. Mater Sci Eng R 2010;71:1–34.
[161] Murata T, Tanoue T, Iwasaki M, Morinaga K, Hase T. J Lumin 2005;114:207–12.
[162] Smet PF, Korthout K, Van Haecke JE, Poelman D. Mater Sci Eng B 2008;146:264–80.
[163] Ju G, Hun Y, Chen L, Wang X, Mu Z, Wu H, et al. Opt Laser Technol 2012;44:39–42.
[164] Wu H, Zhou G, Zou J, Ho C-L, Wong W-Y, Yang W, et al. Adv Mater 2009;21:4181.
[165] Wang Q, Ding JQ, Ma DG, Cheng YX, Wang LX, Jing XB, et al. Adv Funct Mater 2009;19:84.
[166] Yu XM, Kwok HS, Wong W-Y, Zhou GJ. Chem Mater 2006;18:5097.
[167] Morrison RT, Boyd RN. Organic chemistry. 3rd ed. New York: Allyn and Bacon; 1973.
[168] Ma G, Yang Y, Chen G. Mater Lett 1998;34:377.
[169] Morita S, Akashi T, Fujji A, Yoshida M, Ohmori Y, Yoshimato K, et al. Synth Met 1995;69:433.
[170] Lo SC, Burn PL. Chem Rev 2007;107.
[171] Luo J, Zhou Y, Niu ZQ, Zhou QF, Ma YG, Pei JJ. 129. Am Chem Soc 2007: 11314–5.
[172] Pu YJ, Higashidate M, Nakayama KI, Kido J. J Mater Chem 2008;18:4183–8.
[173] Zhou Y, He QQ, Yang Y, Zhong HZ, He C, Sang GY. Adv Funct Mater 2008;18:3299–306.
[174] Choa MJ, Jina JI, Choia DH, Kimb YM, Park YW, Jub BK. Dyes Pigments 2009;83:218–24.
[175] Huang J, Li C, Xia YJ, Zhu XH, Peng J, Cao Y. J Org Chem 2007;72:8580–3.
[176] Oldham WJ, Lachicotte RJ, Bazan GC. J Am Chem Soc 1998;120:2987–8.
[177] Robinson MR, Wang SJ, Bazan GC, Cao Y. Adv Mater 2000;12.
[178] Chen ACA, Culligan S, Geng YH, Chen SH, Klubek KPK, Vaeth M. Adv Mater 2004;16:783–8.
[179] Zhao L, Zou JH, Huang J, Li C, Zhang Y, Sun C. Org Electron 2008;9:649–55.
[180] Sun YH, Zhu XH, Chen Z, Zhang Y, Cao Y. J Org Chem 2006;71:6281–4.
[181] Kulkarni AP, Tonzola CJ, Babel A, Jenekhe SA. Chem Mater 2004;16: 4556–73.
[182] Ho CL, Wong WY, Gao ZQ, Chen CH, Cheah KW, Yao BZ, et al. Adv Funct Mater 2008;18:319–31.
[183] Zhou GJ, Wong WY, Yao B, Xie ZY, Wang LX. Angew Chem Int Ed Engl 2007;46:1149–51.
[184] Barker CA, Zeng XS, Bettington S, Batsanov AS, Bryce MR, Bee A. Chem Eur J 2007;13.
[185] Huang J, Liu Q, Zou JH, Zhu XH, Li AY, Li JW. Adv Funct Mater 2009;19:2978–86.
[186] Cao XB, Wen YG, Guo YL, Yu G, Liu YQ, Yang LM. Dyes Pigments 2010;84:203–7.
[187] Wang Z, Lu P, Xue S, Gu C, Lv Y, Zhu Q, et al. Dyes Pigments 2011;91: 356–63.
[188] Diaz-Garcia MA, Fernandez Da Avila S. Appl Phys Lett 2002;81(21):3924–6.
[189] Tang CW, Van Slyke SA. Appl Phys Lett 1987;51:913.
[190] Adachi C, Tokito S, Tsutsui T, Saito S. Jpn J Appl Phys 1988;27:713.
[191] Adachi C, Tokito S, Tsutsui T, Saito S. Jpn J Appl Phys 1988;27:L269.
[192] Tang CW, Van Slyke SA, Chen CH. J Appl Phys Lett 1989;65:3610.
[193] Heil H, Steiger J, Schmechel R, Von Seggerm H. J Appl Phys 2001;90:10.